Characterization of Intertidal Geomorphology Based on Multi-scale Analysis of Airborne LiDAR Data

by

Peter Andrew Horne

A Thesis Submitted to
Saint Mary's University, Halifax, Nova Scotia
in Partial Fulfillment of the Requirements for
the Degree of Masters of Science in Applied Science.

August 29, 2013 Halifax, Nova Scotia

Approved: Dr. Cristian Suteanu
Associate Professor,
Geography Department / Environmental Science Program, Saint Mary's University

Approved: Dr. Danika Proosdij
Professor,
Geography Department,
Saint Mary's University

Approved: Dr. Joern H. Kruhl
Professor,
Tectonics and Material Fabrics, Technical University of Munich

Approved: Dr. Sageev Oore
Associate Professor,
Mathematics and Computing Science Department,
Saint Mary's University

Date: August 29, 2013

Characterization of Intertidal Geomorphology Based on Multi-scale Analysis of Airborne LiDAR Data

by Peter Andrew Horne

Abstract

Coastal environments are influenced by geomorphic processes operating at different temporal and spatial scales (wave action, tides, vegetation, ice, tectonic changes Characterizing coastal environments often relies on the use of multi-scale analysis methods. However, these methods have been usually applied to coastal environments by intersecting them with a plane at a certain elevation, or by interpreting a coastline from aerial imagery, without specifying the selected elevation. This practice relies on the assumption that one studies a 3D self-similar isotropic system for which the results are independent of the elevation chosen. With the use of LiDAR derived Digital Elevation Models (DEM) the present study showed the elevation dependence of the results of multi-scale analysis on the Avon Estuary and subsections within it. The thesis also assessed the implications that interpolation methods have for multi-scale analysis and highlighted the importance of specifying the interpolation method used in such studies.

August 29, 2013

Table of Contents

List of Abbreviations Used

ALS	Airborne Laser Scanning
CHS	Canadian Hydrographical Services
CVG28	Canadian Geodetic Vertical Datum 28
DEM	Digital Elevation Model
GIS	Geographic Information Systems
GPS	Global Positioning System
HHWLT	High High Water Large Tide
IDW	Inversed Distance Weighting
IMU	Inertial Measurement Unit
LiDAR	Light Detection and Ranging
LPS	Last Partial Step
MP_SpARC	Maritime Provinces Spatial Analysis Research Centre
RMSE	Root Mean Square Error
RTK	Real Time Kinematic
SIM	Slit Island Method

Acknowledgments

I would first like to thank my two advisors. I would like to thank Dr. Cristian Suteanu for all his mentorship over the years. Dr. Suteanu has forever changed the way I perceive the world. Dr. Danika van Proosdij provided me with my first introduction into Geomatics, which has been a great tool for understanding the natural landscape.

I would like to acknowledge the Applied Geomatics Research Group at the Nova Scotia Community College for collecting the LiDAR data and for conducting the ground validation survey. The acquisition of LiDAR was funded by NS Department of Transportation and Infrastructure Renewal, NS Department of Agriculture, Resource Stewardship, Land Protection Section and Saint Mary's University.

I would like to thank Greg Baker, Kevin Garroway and Travis Vale for all their guidance. Lastly, I would like to thank my wife Tiffany and family for all of their support during this journey.

Chapter 1 Introduction

1.1 Background

The topography of coastal environments is affected by a number of processes including hydrodynamic processes, sedimentary processes, vegetation, and ice formations; each of these processes can act over a range of scales. When characterizing these environments it has proved useful to apply methods that evaluate a landscape over a range in scales so that the scaling properties of the landscape can be considered, this can help link form with process. Multi-scale analysis methods, which preform analysis over a range in scales, have been successfully applied to coastal environments, providing a quantitative characterization of the spatial variability of coastlines within marsh boundaries (Schwimmer, 2008), shoreline patterns (Dai, et al. 2004) and evaluating the length of coastlines as they relate to the scale of measurements (Mandelbrot, 1967). Quite often these studies focused on the coastlines that were delineated from satellite imagery, aerial photography, topographic maps and ground based surveys (Dai, et al. 2004; Schwimmer, 2008; Wang, et al. 2007). The practice of delineating coastlines from these forms of imagery and survey data can result in the boundary representing the coastline, which may be performed at a multitude of elevations. This is depending on how one defines the coastline and the inherent effects of the imagery being used. Applying multi-scale analysis to undefined elevation relies on the assumption that the irregularity is independent from elevation. This means that at any given elevation the irregularity of the feature would be the same. This study questions the above assumption by applying fractal analysis, which is a type of multi-scale analysis, not to one, but rather to a series of

different elevations from a high resolution Digital Elevation Model (DEM). An explanation of fractal analysis is provided in the next chapter along with an overview of multi-scale analysis.

There have been a number of advancements within remote sensing over the past decade, but the use of Light Detection and Ranging (LiDAR) systems for the generation of high resolution DEM has developed into wide-spread commercial use (Goulden, 2009). A more in-depth review of LiDAR and DEM interpolation is presented in chapter 3. Applying LiDAR to coastal environments such as inter-tidal zones allows for these environments to be assessed over a much wider scale range than before. In this study the LiDAR data improved the resolutions of the DEM from the previously available data from 20 m to 1 m. This increased resolution allowed for channel networks within the mud flats and mega ripples within tidal bars to be distinguished and characterized in the analysis. There have been a number of studies that have assessed the influence of interpolation methods on morphology and their effects on DEM accuracy (Gou at al., 2010, Bater and Coops, 2009, Aguiler, 2005). However there is a currently a gap in the literature on the influence that interpolation methods have on fractal analysis of coastal environments. This study investigated if the type of interpolation method used would influence the result of fractal analysis by preforming analysis on a series of DEM from the same data set using different interpolation methods.

1.2 Organization of the Thesis

There are six chapters within this thesis. The present chapter provides an introduction to the research, a list of objectives that the research aims to investigate, and finally a review of the methodology used.

Chapter 2 presents a literature review of the research that has been done within multi-scale analysis and advancements in technology as they relate to coastal geomorphology and inter-tidal zones.

Chapter 3 provides additional information into the operation and functionality of LiDAR and the generation of high resolution DEM from LiDAR data, outlining the benefits and limitations of this method.

Chapter 4 evaluates the elevation dependence of scaling properties within the inter-tidal zone of the Avon Estuary. This chapter is a published paper in the June 2013 Volume 29 issue 3 of the Journal of Coastal Research (JCR). The author of this thesis was responsible for the collection of the data, analysis as well as being the primary author of the paper.

Chapter 5 assesses the impact that gridding algorithms have on applying the Slit Island Method (SIM), which is a type of fractal analysis, to a DEM.

Chapter 6 applies the Slit Island Method (SIM) to separate subsections of the Avon Estuary in order to assess the system from five distinct regions within the Avon Estuary.

Chapter 7, the final chapter, provides a summary and discussion of the research and highlights the need for future research within this topic.

1.3 Objectives

The goal of this research was to characterize the scaling properties of tidal bars and mud flats within the inter-tidal zone of the Avon Estuary. A definition of scaling properties is provided in chapter two. The main objectives of this research were to:

- Asses if the tidal bars within the inter-tidal zone of the Avon Estuary are 3D

self- similar or if the scaling properties are elevation dependent.

- Determine if the interpolation algorithms used in the generation of the DEM have an effect on the characterization of scaling properties within an intertidal zone.
- Determine how and to what extent the form of tidal bars can be linked to the processes based on their scaling properties.
- Asses the use of Slit Island Method for feature identification and extraction utilizing high resolution DEM within an inter-tidal zone.

1.4 Study Area

The DEM which was used to assess the scaling properties of tidal bars and mud flats comes from the Avon Estuary, which is a part of the Minas Basin within the Bay of Fundy. The Avon River has a causeway that was constructed in the 1970's and has altered the flow of water through the estuary, which is limited by a tide gate (van Proosdij et al., 2009). There are two other major river systems that flow into the Avon Estuary: the Kennetcook and the St. Croix Rivers. The rate of flow into the Avon Estuary from St. Croix has also been altered by the construction of a hydroelectric facility upstream on the St. Croix River. The Avon and the St. Croix make up about 64% of the drainage basin within the Avon Estuary (van Proosdij, et al. 2005).

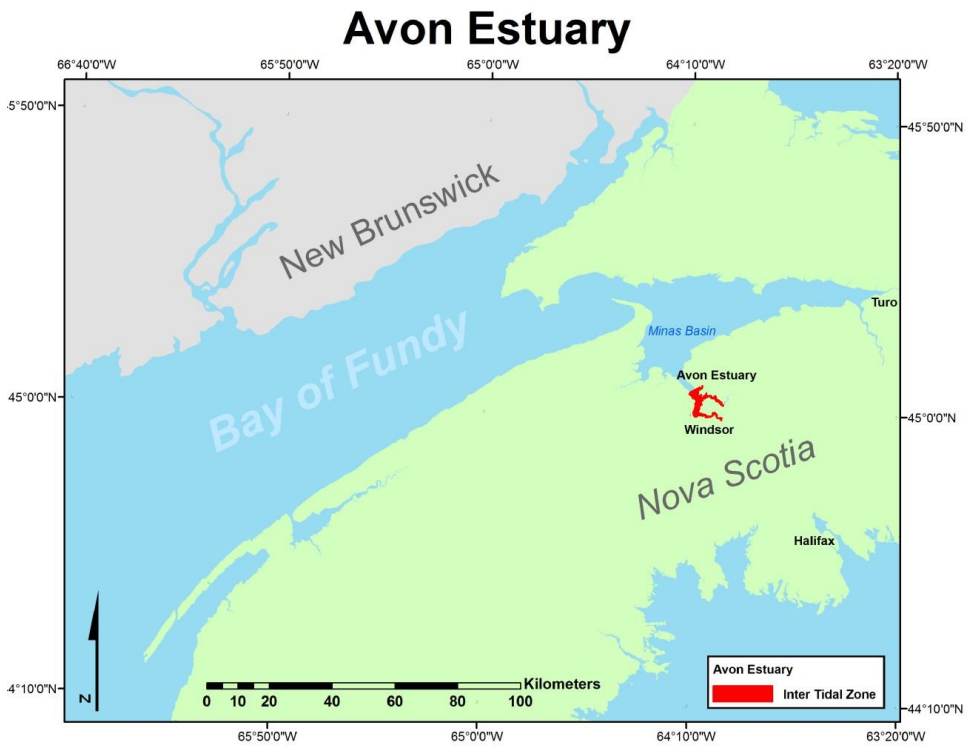

Figure 1.1 The inter-tidal zone of the Avon Estuary (highlighted in red) is found within the Minas Basin near Windsor, Nova Scotia, Canada. The study area itself belongs to the Bay of Fundy, which lies between Nova Scotia and New Brunswick, CAN and Maine, USA.

The Avon Estuary is around 2 km wide near the Windsor causeway and expands up to 2.5 km just above the mouth of the Kennetcook River. At the mouth of the Avon Estuary the width has expanded to around 6km.

There are a number of features that make up the inter-tidal zone of the Avon Estuary such as tidal bars, sand bars, ripples, mega ripples, mud flats and salt marshes. The existence of different types of features within the study area, occurring within different elevation ranges, makes it an ideal study area to evaluate the impact elevation has on the fractal dimension within coastal environments.

1.4.1 Geomorphology of the Avon Estuary

Along with strong tides, the topography of the Avon Estuary is also being influenced by hydrodynamic and sedimentary processes, vegetation, sediment composition, anthropogenic structures and ice formations (van Proosdij., et al. 2006). The bed formation of the inter-tidal zone is characterized by four main types of sediment: sand, mud, gravel and a mixture of mud & gravel. The elongated tidal bars that are formed from sand have been known to produce ripples and mega ripples (van Proosdij., et al. 2006; Pelletier &McMullen, 1972). There is a higher concentration of mega ripples at the upper limit of the Avon Estuary to just south of the Kennetcook River. The ripples are found in tidal bars south of the Kennetcook River and large mud flats dominate the tidal rivers and upper portion of the Avon Estuary. Some of the mudflats have visible channel networks and vegetation, especially near the causeway in Windsor.

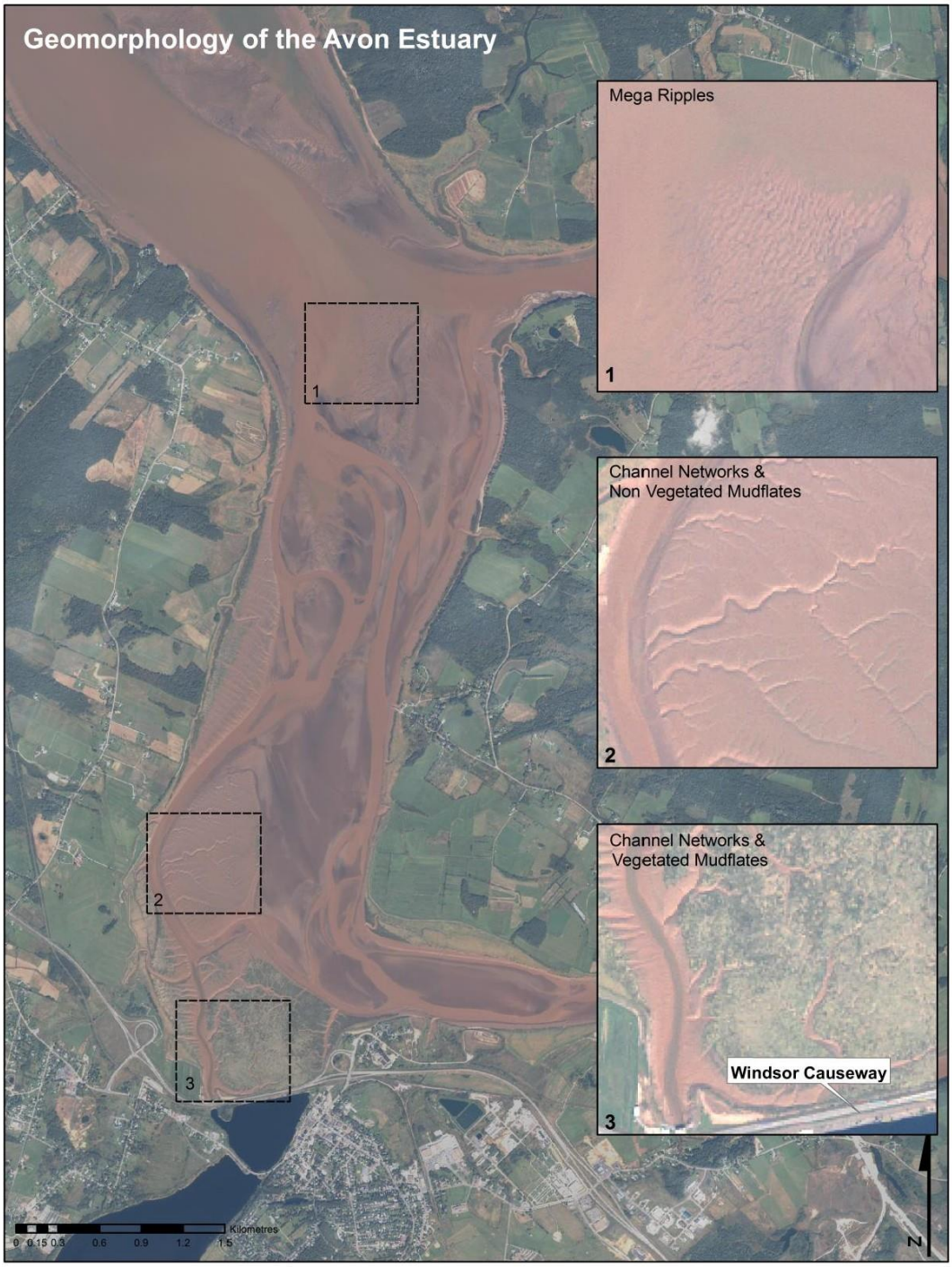

Figure 1.2 Geomorphic features within the Avon Estuary as shown on an Ikonos imagery from September 9,2007. Examples of three distinct features found on mud flats within the Avon Estuary: mega ripples, channel networks and vegetated mudflats.

1.4.2 Anthropogenic Structures

In addition to natural processes, the Avon Estuary is also being affected by two main artificial features, dykes and the Windsor causeway, which have both altered the natural flow of water and the development of salt marshes in the region. The dykes were mainly constructed over the last 350 years, which have altered the natural flow of water and limited the saltmarshes within the estuary. The Windsor causeway was constructed between 1969 and 1970 and has acted as a catalyst for the production of salt marshes within the region. The mud flats around the Windsor causeway have been present since 1858; however, it wasn`t until after the construction of the causeway that the sedimentation rate within the Windsor mud flats increased substantially (van Proosdij, 2007).

1.4.3 Sedimentation

The Bay of Fundy and particularly the Avon Estuary has a high level of suspended sediment during flood waters. The recorded suspended sediment levels range from 100 $mg \cdot l^{-1}$ to 1,700 $mg \cdot l^{-1}$ (Daborn et al., 2002; van Proosdij, 2007). In 1975 and 1976 the rate of sedimentation on the mud flats at the Windsor causeway was measured at 1 to >14 cm per month with an average sedimentation rate of 5 cm per month (van Proosdij, 2007; Amos, 1977). The Avon Estuary has high amounts of sedimentation due to the presence of vegetation within the mudflats, which slow the velocity of water causing the suspended sediment to be deposited (van Proosdij, 2007). Another major influence on the rate of sedimentation and redistribution of sediment are the ice formations which dominate the landscape for approximately 3 months a year.

1.4.4 Ice Formations

The inter-tidal zone of the Avon Estuary within the winter months is covered with snow and ice. The ice formations in the Avon Estuary are commonly known as ice cakes. The ice formations are variable, however they are typically around 2.5 m high and 4 m wide (van Proosdij, 2007). The presence of ice cakes within the region can appear and disappear within a few tidal cycles. When ice blocks build up in channel networks they can alter the pattern of flow and sedimentation rates. They contain high amounts of sediment and plant material and have been linked to the spread of vegetation within the Avon Estuary (van Proosdij, 2007).

1.4.5 Vegetation

Vegetation did not appear on the Windsor mudflats until 1981 and was likely introduced by rafted ice, which previously formed over an area of vegetation and transported plant rhizome material, which started the colonization of the mud flats around the Windsor causeway (van Proosdij & Townsend, 2006). In 1992 the colonization rate of *Spartina Alterniflora* began to experience exponential growth resulting in the mudflat surface area increasing from 41,000 m2 in 1995 to 390,000 m2 by 2001 (van Proosdij, 2007). The high marsh, which is above the mean high water level vegetation, is dominated by Spartina patterns. Whereas the low marsh, which is between the mean high water and the high water level of neap tides vegetation, is almost completely dominated by *Spartina Alterniflora*.

1.4.6 Tides

The Bay of Fundy is renowned for its semi-diurnal tides that can exceed a tidal range of 16 m. The highest tide was recorded at Bruntcoat Head within the Minas Basin at a height of 16.3 m (van Proosdij, 2007). The tidal range within the Avon estuary is around 8.2 m Canadian Geodetic Vertical Datum 28 (CGVD28) during neap tides and 15.6 m during spring tides (van Proosdij, et al.2005). The Higher High Water Large Tide (HHWLT), which is the average of the highest high water levels, is at an elevation of 7.57 m geodetic datum and was chosen as the upper elevation limit within the study. During high tide within the upper portion of the Avon Estuary the Windsor mud flats are completely submerged with only the tops of the vegetation remaining visible. In addition to the large tides the Avon Estuary also has strong currents that are capable of moving large amounts of sediment. In 1980 measurements of the current velocities with the Avon Estuary ranged from 0.6 to 1.7 m*s-1 with the lower velocities occurring at the mouth of the estuary and the higher velocities at the head (Lambiase, 1980; Pelletier &McMullen, 1972).

Figure 1.2 Images of High and Low of the Windsor mud flats. High tide image was taken at 3:11pm June 19th 2011 and the low tide image was taken at 10:30am on June 19th 2011.

Chapter 2 Literature Review

Scaling aspects of geomorphology and multi-scale analysis methods for characterizing coastal environments will be reviewed in this section. In addition, an overview of the use of fractal analysis for characterizing coastal environments will be given along with a discussion regarding implications of not considering elevation when assessing 2D contours. A review of advancements in remote sensing technology, particularly Light Detection and Ranging (LiDAR), that have enabled higher resolution DEM used in a multi- scale analysis have been provided in section 2.5. A more in-depth review of LiDAR will be presented in the next chapter along with a review of the gridding algorithms that were used in this study.

2.1 Scaling Issues in Geomorphology

Landscape morphology is often the result of many complex interactions of processes operating over a range of scales, and characterizing the change in complexity with change in scale can help link form with process (Andrle, 1994). Understanding scaling behaviours of geomorphic systems can lead to improved predictions in the development of geomorphology (Family, Vicsek, 1991). However, identifying a suitable method for this characterization will depend on the type of data and the features that are being analyzed. In the case of coastal environments such as inter-tidal zones there are often a number of processes that can affect the evolution of surface morphology from tidal forces, hydrodynamic forces, mass movement of shore banks, and sedimentation, to ecological factors. Each one of these processes can influence the development of coastal

environments over a range of scales. It is important to apply a method that enables a scale range to be considered when trying to characterize forms and processes from surface morphology

2.2 Multi-Scale Analysis

Since geomorphic landscapes are formed from a number of processes acting at different scales, it is important to apply a multi-scale approach to determine the scale dependence of features within the study area. There have been a number of studies to date that have applied multi-scale analysis methods to the characterization of coastal shorelines and coastal morphology (Dai, et al., 2004; Gao, 2009; Schwimmer, 2008). These environments can be studied two and three dimensionally using such data sources as DEM, contour lines, air photography and satellite imaging; they can also be studied using time series like profile lines.

When applying multi-scale analysis methods to time series data one must consider data stationarity. If the statistical properties of the data set do not change over time then the time series is stationary (Nason, 2006). Non-stationary time series can be more difficult to analyze, but often there are stationary segments within non-stationary time series, and these segments can be analyzed individually (Olsen, et al., 2007).

When applying multi-scale analysis methods to two and three dimensional data sources, this type of analysis is capable of characterizing complex shapes and quantitatively describing scaling properties. Identifying the scaling behaviour, which characterizes how a geomorphic feature's shape varies with scale, would be valuable for determining the optimum resolution of pixel and point based data sources used in Geographical Information System (GIS) or Remote Sensing (RS) applications (Goodchild, et al., 1980,

Sun., et al., 2006).

2.3 Fractals

Symmetry is usually thought of in terms of reflection, translation and rotation. Fractals are a fourth form of symmetry, as they possess some level of self-similarity. Self-similarity refers to objects that are the same under magnification. Objects that are self-similar are composed of copies of themselves at finer scales (Carr, 1997). A fern leaf is an example of this as the fern leaf is similar to the stem which is similar to the whole fern itself. This relationship is known as scaling symmetry or scale invariance. Self-affinity is similar to self-similarity except the x and y axes are scaled differently in order to observe the self-similarity of the object (Sung, Cheng, 2004). An example of this would be a vertical exaggeration, applied to a profile line. Fundamental to fractal geometry is the fractal dimension (D) which describes the scale invariance and amount of irregularity in a data set (Gilbert, 1989). The fractal dimension provides information about the characteristic of the surface being analyzed. For two- dimensional data, if a feature has a fractal dimension of one, then it is linear-like; if it has the dimension two, this means that it is mathematically plane filling (Mark, Aronson, 1984). When characterizing surface morphology, fractals are often used because the invariant properties of fractal sets make them an attractive method for analyzing topographic profiles or contours. Fractal geometry is better suited for describing the irregularity or fragmentation of the shape of natural landscape than traditional Euclidean geometry (Sun, et al., 2006). In geomorphology the fractal dimension is primarily used as a descriptive means for the characterization of surface roughness within the topography (Baas, 2002).

Fractal dimensions of geomorphic surfaces can be derived from two-dimensional

datasets, using contour lines and cross sectional profiles, or three-dimensionally using DEM (Burrough, 1981). There are many methods for determining the fractal dimension of geomorphic systems, and the choice of the methods is dependent on the type of data being analyzed. An important question is whether the data set are self-similar or self-affine. Since geomorphic landscapes can be measured based on changes in horizontal and vertical properties, it is important to review methods of characterizing the self-similarity and self- affinity properties of geomorphic systems. It has been noted in the literature that methods for determining fractal dimension have their theoretical and practical limitations and that not all fractal analysis methods will yield the same result for the same data set (Roy, et al. 1987, Sun et al. 2006, Tate 1998). The following section reviews four of the main fractal methods that could be used in the analysis.

2.4 Methods for Deriving Fractal Dimensions

2.4.1 Divider Method

The divider method has often been used for the evaluation of coastlines (Mandelbrot 1967, Goodchild 1980). The divider method was introduced in Mandelbrot's historical paper on assessing the length of the British coastline over different scales. Following Richardson's studies (1961), he addressed the relationship between the scale used in measurement and the resulting length of the coast line. The divider method is normally applied to two dimensional data that are thought to be self-similar (Andrle, 1996). It performs measurements of the length of a curve using different step sizes of the divider. The total length is determined from $\mathbf{L(}s\mathbf{)=s\ n(}s\mathbf{)}$ where s is the step size and **n** is the number of steps. The fractal dimension is acquired from the following equation:

$$L(s) = \lambda\, s^{(1-D)} \qquad \text{(Eq. 2.1)}$$

Where L(s) is the total length, λ is a constant, and s is the step size. The exponent D is acquired from log-log plots applied to data corresponding to the above equation.

The divider method is influenced by the resolution of the image being analyzed, because the resolution controls the minimum size of the divider step that can be used. With advancements in the resolution of remote sensing data, this method could yield more reliable interpretations of geomorphic features than previously studied, as smaller step sizes could be applied. It is important to note that when applying the divider method, the last step should end at the end of the feature. Step sizes that do not provide a close-to-zero value are known as the Last Partial Step (LSP), and will introduce errors into the interpolation. One method to avoid this introduction of error is to ignore those steps that do not end with a value lower than a selected threshold. This leads to a decrease in the amount of data being interpreted, however rounding LPS values can lead to errors and biases in computation (Suteanu, C., 2000). Both of these solutions for LPS have their challenges associated with them and should be considered before performing any analysis.

2.4.2 Triangular Prism

The triangular prism method was developed in order to calculate the fractal dimension of topographic surfaces by making use of a DEM (Clark, 1986, Sun, et al., 2006). The triangular prism method uses a DEM in a raster form by creating a series of grids across the DEM at increasing step sizes determined by the scale factor. The elevation data at each corner of the cell is used to interpolate a centre value. The cell is split into four

triangles dependent on the centre value and the surface area of the cell is calculated from the four triangles. The fractal dimension is determined by plotting a log-log graph of the changes in surface area as the scale factor is increased (Clark, 1986). One of the downsides to this method is its sensitivity to artifacts in data, so an assessment of the image for noisy pixels should be performed prior to applying this method (Qiu, 1999, Sun, et al., 2006).

2.4.3 Box Counting

Box counting has been a proven method for determining fractal dimensions within geomorphologic systems (Dai, et al., 2004, Kojima, et al., 2006). This method is applicable for self-similar as well as self-affine patterns (Legendre et al., 1994) and can be performed on two-dimensional data such as contour and profile lines representing geomorphic environments. There is also a modified version of box counting used to analyze three-dimensional data such as DEM (3D box counting).

The method relies on counting the number of cells occupied by the structure being analyzed and assessing the way in which this number changes with the size of the cells used to cover the analyzed feature. A grid of a set cell size is overlaid on the feature and the number of cells the feature occupies is recorded for that cell size. The grid cells are then increased in size by the scaling factor and the cells occupying the feature are recorded again. It is this relation between the number of occupied cells and the cell size that is assessed.

Like most multi-scale analysis methods, the results from box counting are affected by image resolution to a substantial extent; the higher the resolution the wider the range in scale that can be considered (Kojima, et al., 2006). In previous studies using box counting

to analyze geomorphic environments such as shore line profiles (Dai, et al., 2004) and fracture patterns of faults (Pérez-López, Paredes, 2006) the base data have been rather coarse, derived from 1 to 50:000 series maps or from 50 and 10 metre resolution DEMs. These studies could be improved by incorporating new methods for high resolution DEM generation in order to improve the range of scale factors being analyzed.

2.4.4 Slit Island Method or Area vs. Perimeter

Slit Island Method (SIM) which is also known as Area vs. Perimeter method is a fractal analysis method introduced in a paper on the fracture surfaces of metals (Mandelbrot, et al., 1984). Unlike other fractal methods, such as the divider method and Box counting, where the user specifies the scale range, SIM is dependent on the scale range of the islands present within the study area.

When applied to DEM, the SIM focuses on the relationship of the area of islands to their perimeter as successive planes are passed through a DEM at different elevations. As the level of the plane passed through the DEM changes, new sets of islands appear and the relationship between the area to the perimeter is established. This is done for each successive pass through the DEM.

Figure 2.1 The Slit Island method establishes a relationship between the areas of islands to their perimeter as successive planes are passed through a DEM at different elevations. The fractal dimension is determined by the slope of a best fit line in a log-log

graph.

The method of finding the fractal dimension is based on the estimation of the power law exponent characterizing the area-perimeter relationship for a set of islands:

Slit Island Method

$$P \propto A^{\frac{D}{2}} \quad \text{(Eq. 2.2)}$$

Where P is the perimeter, A is the area, and D is the fractal dimension.

The method is valuable when utilizing large data sets as it is very robust; however it is not able to detect sub-populations with different fractal values within the data (Suteanu, 2000). The process of performing the SIM is similar to the actual tidal process, as the SIM analyzing the actual islands that form as a plane is passed through a surface, for a given elevation, which is similar to the islands that form as the tide passes through the estuary. In the inter tidal zone, as the tide level acts as the plane, when it decreases there is an appearance of tidal bars and mud flats and these are assessed using the SIM. Applying the SIM to this environment would allow for the characterization of the scale dependence of tidal bars and mudflats. Another benefit of applying the SIM to the study area is that it is also able to be readily applied within Geographical Information Systems (GIS). These two reasons make it an attractive method for this study.

2.5 Advancements in Technology

Geographic Information Systems and Remote Sensing data have improved the ability to analyze both spatial and temporal geomorphic data (Walsh, et al., 1998). The advancements in the acquisition of remote sensing data have improved our ability to

analyze topographic surfaces based on elevation, terrain surface shape, topographic position, topographic context, spatial scale and landform (Dend, 2007). Assessments of these factors come from Digital Elevation Models which are dependent on the point spacing of the survey data used to generate the DEM. Larger point spacing results in coarser DEMs, which limits the range in scale at which the data can be analyzed for feature identification. When applying multi-scale analysis methods to feature extraction from topographic data, the resolution of the data is the limiting factor, as it controls how fine a scale can be applied(Walsh, et al., 1998).

The main advancement in remote sensing that has led to the quantitative analysis of the geomorphic environment for the understanding of scale dependence processes is the development of Light Detection and Ranging systems (LiDAR) (Glenn, et al., 2006). The data from LiDAR can provide resolution of sub metre for topographic information with accuracy of up to 50 cm in the horizontal and 20 cm in the vertical direction (Hopkinson, et al., 2001). LiDAR, as referred to in this thesis, refers to Airborne Laser Scanning (ALS), which uses a laser range finder, an Inertial Measurement Unit (IMU) and a Global Positioning System (GPS) to determine the position of the returns in three dimensional space. One of the main advantages of LiDAR systems over traditional surveying methods is that they can easily collect data in remote and possibly dangerous environments. This technology would be ideal for surveying in tidal environments such as the Bay of Fundy that have limited low tide exposure and are difficult to navigate due to the high amount of mud. A more in depth review of LiDAR is presented in the ensuing chapter.

It is important to note that the use of DEM in scaling analysis, whether from LiDAR or more traditional survey practices, could have questionable results, if errors are

introduced, such as GPS errors, IMU drift, human error, etc. Therefore, errors within the data collection and DEM generation methods are assessed and accounted. If left uncorrected the error could propagate through the analysis (James et al, 2007). It would be particularly beneficial to assess the error within LiDAR digital elevation models and their sources of error before performing any scaling analysis. There is a gap in the literature on the effects that interpolation method used to produce a DEM have on scaling analysis. Applying a series of different interpolation methods before performing scaling analysis would help to quantify the effects that gridding choices play.

2.6 Discussion

There have been a number of methods for the characterization of geomorphic landscapes presented in this review and the common theme throughout is that all of these methods are affected by the resolution of the data being analyzed. Any of the above methods would be improved with the use of high resolution data. LiDAR data collected over a few hours can provide a high resolution DEM over a large area. The short collection time required to survey large areas makes it an ideal data source when applying multi-scale analysis methods characterizing geomorphic landscapes that are rapidly evolving such as the Avon Estuary. The effect of interpolation method used in producing a DEM should also be assessed as the choices used to assign elevation information to areas without known points can change the variability within the systems and influence scaling properties. The influence that interpolation methods have on variability of a DEM would affect the reliability of the results. The next section provides additional information about LiDAR and DEM generation techniques that have been utilized in this study.

Chapter 3 The Use of Light Detection and Ranging Systems in the Generation of Digital Elevation Models

3.1 Digital Elevation Model Background

A Digital Elevation Model (DEM) is an array of elevation values representing a topographic surface which has been generated from a number of known points and the surface between known points has been interpolated (Lo, Yeung, 2002). The resolution of a DEM affects the reliability of the analysis preformed on it; for instance, coarse data sets can model stream flow in the wrong direction whereas higher resolution DEM can provide more accurate flow direction, as they can account for differences in elevation which are not represented in coarse DEM.. DEM were always data intensive computer models, which limited the resolutions of the DEM in the past as the file size required for higher resolution was exceeding the available hardware limits. As computer technology advanced through the 1980s to 2010s they were better equipped to handle more information and this allowed for computer based photogrammetry, Synthetic Aperture Radar (SAR) interferometry and Airborne Laser Scanning (ALS) systems to produce higher resolution digital elevation models. With increased computing power, automated DEM generation procedures from more traditional practices such as photogrammetry are now able to produce DEMs with sub-metre accuracy (Schiefer, 2007). Generally the most widely available DEM are from provincial sources which have been produced from photogrammetry and have a resolution of around 20 metres, which is now considered low resolution. In addition to the low resolution photogrammetry also had lengthy generating times associated with them. There was a need within the industry to improve on the resolution of DEMs along with generation times, as improved resolution would

lead to improved confidence in the analysis carried out on DEM. The development of Light Detection and Ranging systems (LiDAR) enabled the production of high resolution DEMs with minimal production times. The resolutions DEMs generate using LiDAR can be at the decimeter level.

3.2 Description of LiDAR

There are five main components to a LiDAR system: a laser range finder, computer, Inertial Measurement Unit (IMU), scan mirror, and differential GPS. The LiDAR system is often housed within an aircraft and is usually operated from a fixed wing aircraft but helicopters are also commonly used for smaller jobs to reduce turning times between flight lines. The laser emits a series of near-infrared pulses which travel through a fiber optic cable to the scan mirror which determines the angle at which the pulse will be emitted from the sensor. The pulse then travels to the scanner to the surface of the ground, back-scatters and part of the pulse is returned back towards the scanner. The time at which the pulse returns to the scanner is recorded (T) and compared against the time the pulse is emitted from the system to determine the range (R) each pulse traveled.

Today more modern systems have the ability to record a series of returns from a single pulse. As the pulse comes in contact with such things as vegetation, if only a part of the pulse makes contact with the surface the remainder will continue to travel on its trajectory until it comes in contact with another surface (Garroway, 2006). The Optech ALS 3100 system which was used in this study has the ability to record four returns from a single pulse. The laser pulse from a standard LiDAR system, such as the Optech 3100,

can range in frequency from 30 kHz to 100 kHz (Chasmer, 2006). The lower the frequency of the laser pulse, the stronger signal sent out. When the frequency of the laser pulse is increased, the signal strength is decreased, but more pulses are emitted per time unit. The trade-off means that at a lower frequency pulse the system can be flown at a higher altitude but fewer data are collected, whereas at a higher frequency the aircraft must be flown at a lower altitude and the system will collect more data. Using a 70 kHz pulse is most commonly used when collecting data for DEM construction because at this rate the laser pulse has enough strength to penetrate the forest canopy and return to the aircraft while still maintaining desired spot spacing determined for the survey.

The IMU measures the altitude of the aircraft, recording the yaw, pitch and the roll. The position of the aircraft is recorded for each pulse. The exact position of the aircraft is necessary in order to derive the angle each laser pulse was emitted from the aircraft. GPS gives the location of the aircraft. This location shows the latitude, longitude and elevation above sea level. There are two GPS associated with LiDAR. One is mounted to the aircraft itself and it gives the location of the laser unit. If you know where the laser is in geographic space coupled with the IMU, you can ascertain the location of the laser pulse when it hits the earth surface as the trajectory from the systems along with the range is recorded. The second GPS is a base station, located over a known point and is used to correct the location of the GPS on the plane. The base station records the error associated with external factors affecting the GPS signal and that offset can be applied to the aircrafts GPS to compensate for these errors. The ionosphere disturbance is one example of external disturbance that commonly affects the GPS and the error is generally the same within the survey range of a LiDAR mission. If you monitor the change in a location over

a known point then the GPS error is recorded. In post-processing, the appropriate correction is used to "fix" the data and make it them accurate as possible. This improves the overall accuracy of the DEM.

3.3 Benefits of LiDAR

The changes that LiDAR has brought to the Geomatics world are staggering. Now large sections of land are surveyed in just a few hours or days with as little as two people. This task would have taken land survey crews months or years to survey with the same point spacing that LiDAR provides with GPS or total stations. In areas where there is tree-cover or lower levels of relief, photogrammetry cannot produce as high accuracy DEM as LiDAR. LiDAR also made surveying in dangerous ground conditions possible. The Avon Estuary is a prime example of this as taking transects with traditional ground survey methods can be difficult and possibly dangerous given the tidal nature and the soft substrate.

LiDAR data can provide high-resolution topographic information with 50 cm horizontal and 20 cm vertical accuracy (Hopkinson, 2001). The vertical accuracy makes it more favourable than photogrammetric methods over accumulation zones of glaciers (Kennet & Eiken, 1997). Having higher vertical accuracy would also be more favorable in inter-tidal zone of the Avon Estuary since being able to detect changes due to sedimentation at a sub metre level would be beneficial for elevation change detection of mud flats and sand bars. The laser pulse also returns an intensity value, which can aid in feature identification along with measurements of the feature; this is a distinct advantage of using LiDAR over other DEM generation methods (Hopkinson, et al., 2001). High resolution DEMs of geomorphic environments can be analyzed using multi scale analysis. The

importance of high-resolution data is at the utmost when applying multi-scale analysis methods to topographic data, as geomorphic processes acting at one scale can be affected by those processes acting at finer and coarser scales (Walsh et al 1998). LiDAR datum provide the high-resolution topographic information that is needed for the quantitative geomorphometric analysis necessary to understand spatial scale-dependent processes (Glenn, N.F., et al., 2006).

3.3 Data Collection

On April 3, 2007 the airborne LiDAR survey of the Avon Estuary was conducted by Laura Chasmer and the author of this thesis with the Applied Geomatics Research Group (AGRG). The LiDAR system that was used was an Optech ALTM 3100. This is a 100 kHz sensor capable of receiving up to four returns per pulse. The system was not designed to penetrate water, so the LiDAR survey was conducted during low tide in order to maximize the area of the tidal zone that could be surveyed. The mission was flown using the specifications in the below discussion.

3.3.1 Survey Specifications

The scan angle was set to 20 degrees. The scan angle limits the swath width. This is important because as the swath width increases it causes the pulse to become more elongated at the higher angle as it contacts the surface. An elongated pulse results in greater uncertainty, as there is no information on where within the pulse the return is coming from, and if the elongated pulse is a terrain of mixed elevations then areas may be over-or under-represented by their elevation value.

The scan frequency was set to 70 kHz, which is at medium range. The frequency

controls how many pulses will be emitted from the LiDAR system at a given time. The higher the frequency the more pulses will be emitted however there is less amount of energy per pulse. This will result in some features not having enough energy in the returns to be recorded if there is absorption of the energy due to the surface type. Since the laser that is used is near infra-red, it is absorbed by water; therefore, in areas of water there are often little to no returns. The LiDAR mission was collected at an air speed of 40 knots and at an elevation of 1200 m. The elevation and the flying speed are important in controlling the point spacing on the ground along with the scan frequency and scan angle. The survey was conducted with 50 overlaps to account for small movements in the aircraft during the survey due to such factors as air turbulence and cross-winds that can make it difficult for the pilot to maintain the flight path.

3.3.2 Ground Validation

The AGRG conducted a ground validation survey of the Avon Estuary on April 3rd 2007, using a dual frequency Leica GPS 530 Real Time Kinematic (RTK) system, which achieved sub decimetre positional accuracy. GPS points were collected throughout the study area on road ways, covering each flight line, and were used to verify the vertical accuracy of the data set within 15 cm.

3.4 Measuring Error within the DEM

The most common approach to assessing DEM accuracy, when comparing locations within the DEM to surveyed points, is the Root Mean Square Error (RMSE) statistic (Wechsler, 2007). However, the RMSE does not provide an assessment of how each cell within the DEM compares to its true elevation. This is mainly due to the fact that the

error within a DEM is often not normally distributed (Garroway, 2009; Goodchild and Gopal, 1989). Nevertheless the RMSE does provide some level of quality assessment for the data, and its findings are valuable when considering overall accuracy of the data.The difference in elevations from the DEM and the surveyed points are taken and then squared. The average of the squared differences is then determined and the square root taken to produce the RMSE for the DEM.

The RMSE was applied in this study to evaluate the accuracy of the DEM that was generated from an April 2007 LiDAR flight over the Avon Estuary. The DEM was validated against survey data collected by the Maritime Provinces Spatial Analysis Research Centre (MP_SpARC) in August 2006. The validation survey data was captured with the use of signal frequency differential GPS and a Leica total station. It is important to note that the validation data are not from the same time period as the LiDAR data and the surface of the non-vegetated inter-tidal zone can fluctuate in the order of metres during this time lapse. However the survey data is from the upper marsh and the amount of fluctuation in topography is considerably less than in the tidal bars.

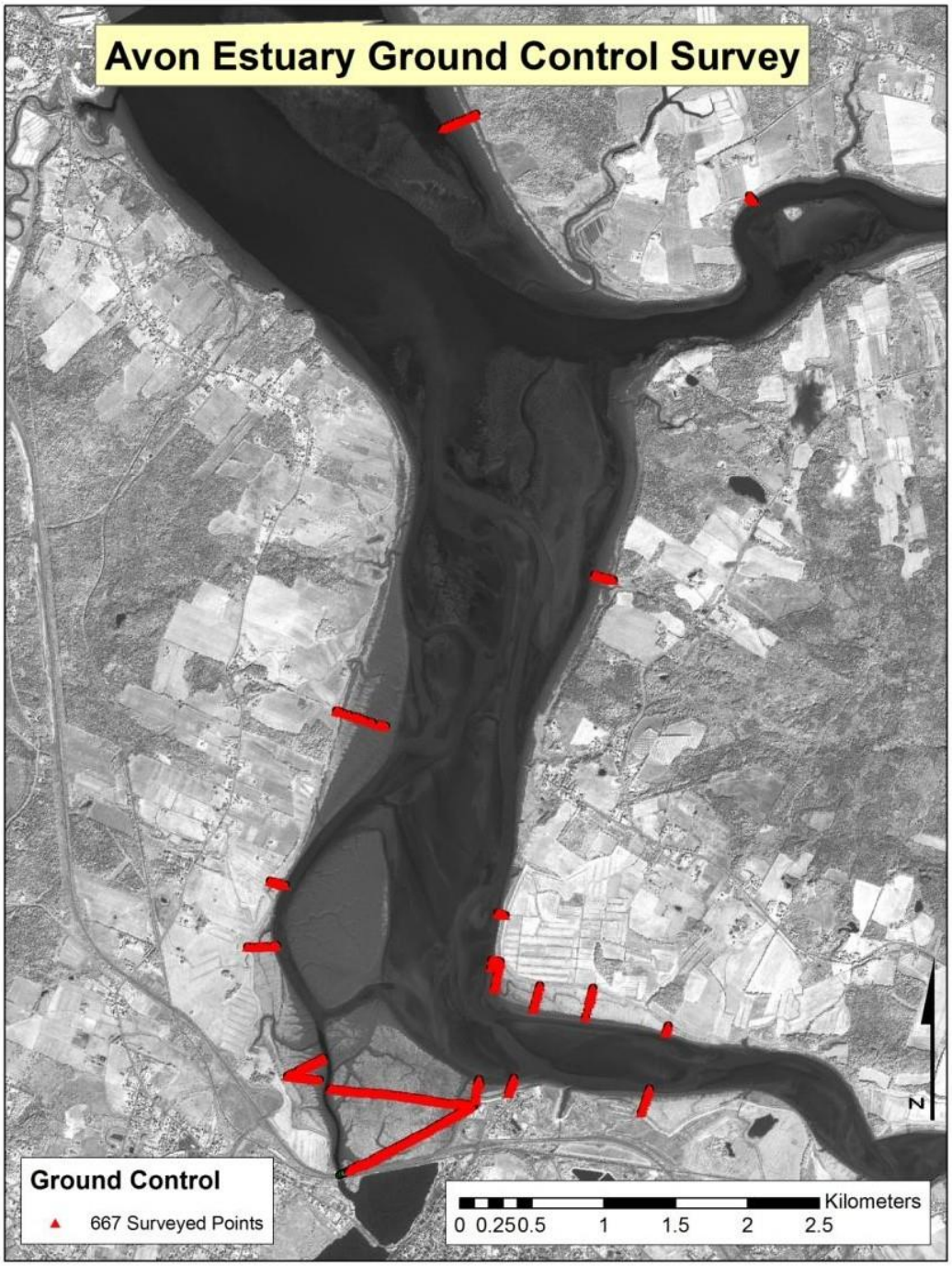

Figure 3.1 Map image of the 667 GPS points and total station points collected throughout theAvon Estuary used to validate the DEM.

There were 667 surveyed points inside of the study area, predominantly around the Windsor mud flats, the banks of the main channel, and the banks of the St. Croix and Kennetcook River. There were also a number of surveyed points that were outside the inter-tidal zone, but within the limits of the LIDAR dataset, which allowed for a more accurate error assessment, as the topography of the surrounding landscape is not subject to the same evolutionary processes as the Avon Estuary and in fact would experience very little change in elevation during the 8 months' time difference between validation survey and LiDAR data collection. The RMSE was calculated for both the survey points within the study area and those that fell outside on more stable ground.

The GPS and total station points that were within the Avon estuary produced a RMSE of 47 cm, whereas the points from the more stable ground from parking lots and tops of dykes produced an RMSE of 26 cm. The accuracy is within the accepted limits of a half a metre and it was determined that the DEM was of good quality for this line of analysis.

Chapter 4 Elevation -Dependent Multi-scale Analysis of a Complex Inter-Tidal Zone

The chapter is a published paper from the June 2013 Volume 29 issue 3 of the Journal of Coastal Research (JCR). The author of this thesis was responsible for the collection of the data, data analysis as well as being the primary author of the paper (Horne, et al., 2013).

4.1 Abstract

Coastal geomorphology is the result of many complex interacting processes operating over a range of scales in space, and multi-scale analysis on relevant scale intervals can help link form with process. Numerous studies focus on lines resulting from the intersection of a plane at a certain elevation with the three-dimensional landscape. However, in most cases, the reason for the choice of the actual elevation is not mentioned, nor at times is the value of the selected elevation even specified. Such an approach relies on the assumption that one studies an isotropic, self-affine pattern for which the irregularity is independent from elevation. The present study questions this assumption by applying fractal analysis not to one, but rather to a series of different elevations relating to tidal stages. The research takes place a macro-tidal estuary, in the Upper Bay of Fundy, Canada where diurnal tides exceed 14 m. The topography of Avon Estuary is influenced by complex interacting factors, including hydrodynamic and sedimentary processes, vegetation, and ice formations, as well as by anthropogenic structures. The area-perimeter analysis method was applied to 0.5 m contour intervals on a digital elevation model derived from a LiDAR survey conducted at low tide. The results show a pronounced and coherent dependence of the fractal dimension

on elevation. Fractal dimensions between 1.2-1.17 are generally associated with sand sediment transport and bedform development at elevational ranges from -5 to -1 m CGVD28. Between D values 1.17 and 1.12 at elevations from -0.5 to 2.5 m CGVD28, vertical accretion processes dominate with bank edge erosion. D values continue to increase above elevations greater than 3 m as vegetation becomes established and stabilizes the intricate tidal creek networks. We show that this approach supports a better understanding of the interacting processes that dominate the area on different ranges of scale.

ADDITIONAL INDEX WORDS: Tidal wetlands, sediment accretion, geomorphology, elevation, Area-Perimeter method, Fractal analysis

4.2 Introduction

The inter-tidal zones dominated by tidal influences are subject to eroding shorelines and continuous redistribution of sediment. Numerous variables govern the evolution of the surface morphology, within inter-tidal zones, such as hydrodynamic and sedimentary processes, vegetation, anthropogenic structures and ice formations. Characterizing the overall shape of the coastline can be problematic, as the relative influence of these variables can dominate at different elevations within the tidal range, resulting in changing rates of sedimentation or vegetative colonization.

Characterizing this type of dynamic coastline geometry requires methods that extend past the use of traditional geometrical methods. Multi-scale analysis methods are capable of characterizing complex shapes and quantitatively describing scaling properties. When characterizing surface morphology, fractal approaches are often applied because the invariant properties of fractal sets make them an attractive method

for analyzing topographic profiles or contours (Dai, *et al*., 2004; Mandelbrot, 1967; Schwimmer, 2008). Fractals are well suited to describe the irregularity or "fragmentation" of the natural landscape that traditional Euclidean geometry cannot (Sun, *et al*., 2006). Fundamental to fractal geometry is the fractal dimension (D), which describes the scale invariance and amount of irregularity in a data set (Gilbert, 1989). There are many methods for determining the fractal dimension of geomorphic systems, and they are applied as a function of the type of data being analyzed (Gao and Xia 1996).

Data sets can be self-similar or self-affine. Features that are self-similar have the same appearance regardless of the scale at which they are viewed. Geomorphic systems are not truly self-similar but may act as such over a range of scale. Self-affinity, on the other hand, is characterized by the fact that features look alike on different scales when the reduction of scale is made with different scaling factors along distinct geometric directions, i.e. scale invariance is obtained through anisotropic changes in scale (Carr, 1997; Sung and Chen, 2004).

Methods for determining fractal dimension have their theoretical and practical limitations, may reflect different aspects of the analyzed patterns, and may produce different results for the same data sets (Ioana *et al.* 1997; Sun *et al.* 2006; Tate 1998). For this reason it is important to consider the method that was used in calculating the fractal dimension when comparing different studies. When fractal analysis methods have been applied to characterizing coastal environments, coastlines have been delineated from aerial photographs and topographic maps often at 1:50,000 to 1:600,000 scales (Dai, *et al.* 2004: Jiang and Poltnick, 1998). Often, this approach may

only portray the coastline from a two dimensional point of view. Most studies refer to coastline patterns without providing information about and reasons for the choice of the particular elevation used to define the coastline (Pan *et al.*, 2003; Wang *et al*. 2009; Sharma and Byrne 2010; Su *et al*. 2011): it is implicitly assumed that the characteristics of the coastline pattern are not elevation dependent. Delineating coastlines only from a two dimensional point of view relies thus on the assumption that one studies a self-similar pattern, for which the irregularity is the same for all elevations. The assumption is particularly consequential for areas with a large tidal range, where the arbitrary choice of the pattern-defining elevation is expected to have no effect on the outcome of the pattern analysis. Our study sets forth to check this assumption, and pursues two objectives.

On one hand, it addresses the question whether coastal patterns in environments subject to large tidal ranges are, indeed, elevation-independent. For this purpose, it applies multi-scale analysis to quantify the "irregularity" of the patterns of intertidal topography in a series of horizontal sections. Our findings show that, in fact, pattern characteristics change significantly with the elevation at which the analysis is applied. A direct implication of this result consists of the recommendation for coastline pattern studies to document the elevation for which pattern characteristics were found; in absence of such specifications, the objectivity and reproducibility value of the studies may be significantly reduced.

On the other hand, we explore the relation between elevation and the quantified degree of irregularity, check its consistency and discuss its possible links with physical processes occurring in the area. Since even subtle changes in pattern irregularity are

quantitatively identified and compared among the different sections, the multi-scale and multi-elevation approach we propose here is shown to provide access to rich information about a tidal environment, which is otherwise difficult to obtain, and to open an expectantly fertile field of investigation of links between forms and their relation to processes. To address these objectives, the patterns of the tidal bars within the Avon Estuary were subject to an analysis based on the Slit Island Method (SIM) (Mandelbrot *et al.* 1984) at half-meter intervals over the tidal range of the Avon Estuary from -5 m to 7.5 m above geodetic datum (CGVD28). The use of a high-resolution DEM enabled all closed contours, which are referred to in this study as islands, with an area over 4 m^2 to be included in the analysis. The area and perimeter of the islands used in the analysis range over 5 orders of magnitude.

4.3 Study Area

The Avon Estuary (Figure 4.1), which is a part of the Bay Fundy in Nova Scotia, is renowned for its semi-diurnal tides that can exceed a tidal range of 14 m (Desplanque and Mossman, 2004). Along with the strong tides the topography of Avon Estuary is also being influenced by hydrodynamic and sedimentary processes, sea level rise, vegetation, anthropogenic structures and ice formations during the winter months (van Proosdij., *et al. 2009).*

The bed formation of the inter-tidal zone is characterized by four main types of sediment: sand, mud, gravel and mixture of mud and gravel. The tidal bars that are formed from sand have produced ripples and mega-ripples (Lambiase, 1980). There is a higher concentration of mega-ripples at the upper limit of the Avon Estuary to just south of the Kennetcook River (Pelletier and McMullen, 1972). The ripples are found in

tidal bars south of the Kennetcook River and large mud flats dominate the tidal rivers and southern portion of the Avon Estuary (van Proosdij, 2007). Some of the larger mudflats have distinct channel networks and vegetation.

In addition to natural processes, the Avon Estuary is also being affected by two main artificial features: dykes and the Windsor causeway, both of which have altered the natural flow of water and the development of salt marshes in the region. The dykes were initially constructed by the Acadians 350 years ago (van Proosdij, 2007), however these were supplemented by dykes and causeways constructed in the 1940s-60s by the Maritime Marshland Rehabilitation Administration (NSDAM 1987). The mud flats around the Windsor causeway have been present since 1858, however the construction of the causeway stimulated significant increases in the sedimentation rate. After the construction of the causeway there was a 90% decrease in cross sectional area, and, with the introduction of vegetation in 1992, an increase in marsh area from 41,000 m^2 to 390,000 m^2 by 2001 (van Proosdij *et al.* 2009). The research focuses on three sections of the Avon Estuary (Figure 4.1): the entire Avon Estuary up to the limit of available data, and two sub sections, the upstream portion and the main channel. The upper portion was selected as the limit of the inter-tidal zone, which is just below the Kennetcook River and extends upstream to the Windsor causeway and to the tidal limit of the St. Croix River. The two sub sections were chosen to investigate the possible influence that tidal rivers may play on the analysis by removing one, and then both rivers from the analysis. Changes in the fractal dimension would suggest that the tidal rivers are different environments then the main channel and should be characterized separately. During low tide there is minimal freshwater drainage within the base of

main thalweg and the entire bed of the upper limit is exposed. The main channel boundary also begins south of the Kennetcook River but extends up to the mouth of the St. Croix River and excludes the river itself. The study is limited to a range of elevations within the Avon Estuary, focusing on the intertidal zone from -5 m which was lowest reliable set of elevations record during the surveyed to the highest high water large tide (HHWLT) level (~7.5 m above CGVD28 vertical datum at Hantsport – Canadian Hydrographic Service Chart 4140 1969).

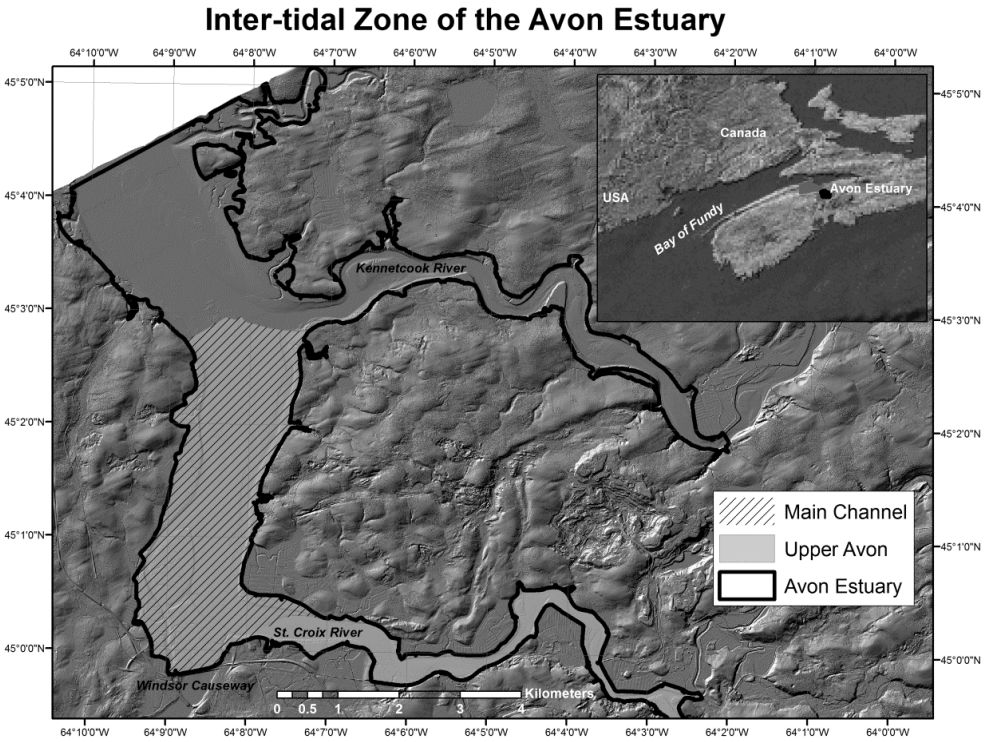

Figure 4.1: Three zones within the Avon Estuary have been chosen for fractal analysis to evaluate the scaling properties of the pattern. The entire Avon Estuary up to the limit of available data was chosen along with two subsets from within the upper portion and the main channel. The upper portion ranges from below the Kennetcook River to the end of the tidal portion of the St. Croix River and is shown as solid lines. The main channel

represented by dashed lines boundary is from below the Kennetcook River to the mouth of the St. Croix River.

4.4 Methods

4.41 Data Collection

LiDAR is based on Airborne Laser Scanning (ALS), which uses a laser range finder to determine the distance from the aircraft to the ground, an Inertial Measurement Unit (IMU) to provide the orientation and heading of the aircraft, along with a Global Positioning System (GPS) to determine the location of the aircraft as each laser pulse is emitted and received from the range finder. Combining the range, GPS and IMU data determine the fix ground co-ordinate of each laser pulse (Hopkinson *et al.*, 2001). LiDAR has been proven to be a valued tool for mapping elevations within tidal environments, as LiDAR data can achieve 20 to 60 cm vertical and horizontal accuracy respectively within tidal wetlands (Athearn *et al.* 2010). It is also important to note that the laser pulse from the LiDAR system returns an intensity value which can aid in the identification of channels, mudflats, streams and delineation of vegetation. In addition to the identification of features, accurate measurements can be made, which is a distinct advantage of using LiDAR over other DEM generation methods that may not allow the identification or accurate measurements of features (Hopkinson *et al.*, 2001). The airborne LiDAR data of the Avon Estuary were collected on the 3rd of April 2007 by the Applied Geomatics Research Group (AGRG) using an Optech ALTM 3100 LiDAR system. Data were collected during low tide (springs) to maximize the exposure of mud flats. It was imperative to collect the data during low tide, as the ALTM 3100 system uses a near infrared laser pulse which is absorbed by water and

often does not return an intensity value strong enough to be recorded if used over water (Goulden, 2009). Since moisture limits the intensity of the return, this perceived weakness within the system is also one of its strengths, as it provides clear delineation of the water surface**.** The survey was conducted using a 20 degree scan angle, a scan frequency of 70 kHz and a 50% overlap in swath width of adjacent flight lines, resulting in a data resolution of 0.5 m. Having the 50% overlap helped to insure data coverage, as each location was surveyed twice and small gaps caused by slight movements within the aircraft during the survey were minimized. Ground validation was conducted by AGRG on the same day using a Leica GPS 530 RTK system which achieved sub-decimetre positional accuracy. GPS points were collected throughout the study area covering each flight line and were used to verify the vertical accuracy of the data set within 15 cm.

4.4.2 Data Preparation

The LiDAR survey was classified into ground and non-ground returns using standard classification algorithms in Terra Scan, an extension of the Bentley Micro station. The ground returns were then exported into a XYZ file format to be used in the production of a DEM of the Avon Estuary. The DEM enabled contours to be produced at 0.5 meter intervals ranging from –5 m to +7.5 m (CGVD28 vertical datum) within the Avon Estuary.

Elevations below –5m returned unreliable results, as artifacts in the data resulting from effects such as that of standing water affected the reliable generation of polygons representing the true landscape. The 7.5 m level was chosen as the upper limit because 7.57 m represents the High-High Water Large Tide (HHWLT) level based on Canadian

Hydrographical Services (CHS) Hantsport tidal station 282 within the Avon Estuary converted to the Canadian Vertical 1928 vertical datum (CGVD28).The contours were generated using the contour feature within ESRI ArcGIS 9.3 3D analyst extension and were then converted to polygons with ET Geowizard's (ET Spatial Techniques) polyline to polygon command Since the polyline to polygon command only converts contour lines that are closed to polygons; all others were discarded from the analysis. This procedure simulates the process of moving a plane through a surface creating islands at different elevations. The polygons that are generated are then compared using the area-perimeter method commonly known as the Slit Island Method (Figure 4.2).

4.4.3 Slit Island Method (SIM)

Slit Island Method (SIM) is a fractal analysis method introduced by Mandelbrot and co-workers in their 1984 paper on fracture surfaces of metals (Mandelbrot et al. 1984). SIM is also known as the area-perimeter method, as it focuses on the relationship of the area of islands to their perimeter as successive planes are passed through a DEM at different elevations. The method of finding the fractal dimension is based on the estimation of the power law exponent characterizing the area-perimeter relationship for a set of islands:

$$P \propto A^{\frac{D}{2}}$$

Where P is the perimeter, A is the area, and D is the fractal dimension.

The fractal dimension can be thought of as a measure of surface roughness considered on a range of scales; surfaces with lower fractal dimension are smoother than those

with higher fractal dimension. For example, lines lying in a plane have a fractal dimension between 1 and 2. A straight line is 1-dimensional, whereas "wiggly", irregular curves have a higher dimension: the stronger the irregularity, the higher the dimension. Theoretically speaking, a curve that would be so irregular as to "fill" the surface would have a dimension D=2. The fractal dimension has been found to be a reliable and convenient way of characterizing and discriminating a variety of shapes, and is successfully applied for the quantitative evaluation of topography (Poljacek *et al*. 2008; Sharma and Byrne 2010; Su *et al*. 2011; Wang *et al.* 2009). Among the fractal analysis methods that are effectively applicable to topography, SIM enjoys important advantages (Suteanu, 2000): it can be reliably established, and it provides robust results. In other words, its outcomes reflect the characteristics (irregularity) of the overall pattern, without being influenced by individual features expressed in various locations. For example, two curves that are equally irregular, even if they are only similar to each other, would be identified as such; on the other hand, if one of the curves became slightly smoother (or rougher), the change in the amount of irregularity would be accurately measured by this method. The pattern characterization is thus performed regardless of local details: what counts is the spatial arrangement of the parts of the curve in relation to its other parts, on different scales. The reliability of the method is reflected in the fact that as long as the above relation between area and perimeter is found and backed by strong correlation, the resulting dimension D characterizes the assessed shapes with high accuracy and high precision (low uncertainty intervals, compared to other methods). The limitations of the method consist mainly of the fact that (i) subsets of islands with different fractal dimensions

cannot be distinguished, and (ii) only sets of closed contours can be approached with this method (Suteanu, 2000). Limitation (i) can be effectively avoided by checking the correlation strength characterizing the area-perimeter relation. On the other hand, limitation (ii) makes the method inapplicable to open loops and line segments. For this reason, one can only benefit from the advantages of the method in circumstances in which islands exist or can be created (e.g. by the intersection of an irregular 3-dimensional surface with a plane).

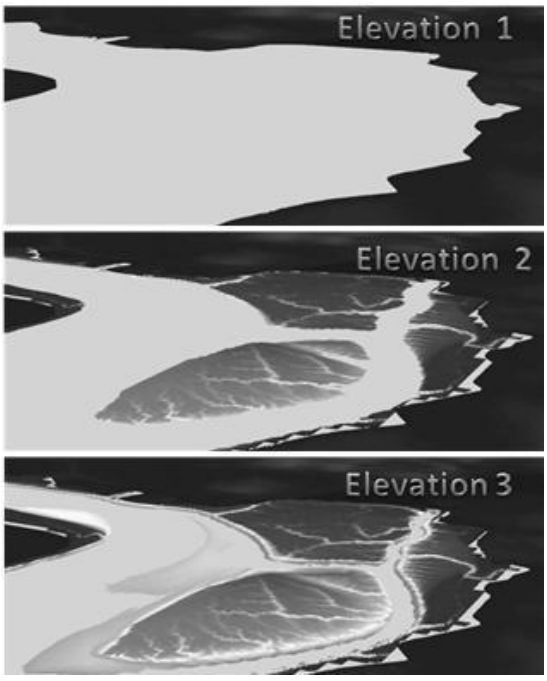

Figure 4.2: The Slit Island method determines the relationship of the area of islands to their perimeter as successive planes are passed through a three-dimensional surface at different elevations. The three elevations show that as the plane decreases in elevation the formations of islands appear. It is these islands that are used within the analysis.

Originally, Mandelbrot *at al*. (1984) introduced SIM as a way of assessing the irregularity of surfaces at the microscopic scale: their goal was to characterize the

roughness of different fracture surfaces in metals. To this end, they produced intersections between the rough surface and planes parallel to the surface, by polishing the surface and assessing the resulting "islands". They applied successive polishing stages, removing more and more material from the surface, which created new sets of islands: some islands grew larger and larger and new islands appeared from one polishing stage to another. Due to the capability of the method of reliably distinguishing even subtle differences among patterns, it was successfully applied to "topographic" surfaces and "islands" and particle clusters of different origin (Almqvist 1996; Droppo and Ongley 1992; Han *et al*.2007; Krummel *et al*. 1987; Pan *et al*. 2003; Yan *et al*. 2011; Zaady *et al*. 2009). In our study, we generate "islands" by intersecting the DEM with a series of horizontal planes. Interestingly, this island generation process, which is usually applied only theoretically, to a model (DEM), has in our case a physical correspondent: the islands generated by the method are actually also produced in reality by the variation in water level in the studied tidal environment.

In this study, SIM was applied to the inter-tidal zone of the Avon Estuary for islands ranging from 4 m^2 to 65,000 m^2. The analysis was limited to a cut off of 4 m^2, which was four times the resolution of the DEM. This limit was chosen to avoid small errors within the DEM caused by slope and the uncertainty within the pulse footprint. The footprint of the laser pulse is around 25 cm when it comes in contact with the ground, and the position of the return within the footprint of the pulse is unknown for each return. The unknown position of the return within the laser pulse results in areas of increased slopes having higher elevation error then points coming

from level terrain (Goulden, 2009). No limit was applied to the maximum size of the analyzed islands.

4.4.4 Interpretation of Geomorphic Features

Intertidal features were identified based on close examination of a 2007 IKONOS panchromatic image with 0.86 m resolution. A multi-spectral image with 2.5 m resolution was used to confirm the presence of vegetation. This research drew heavily from field observations and a detailed sedimentological interpretation of the estuary reported in van Proodij, 2007.

4.5 Results

4.5.1 Elevation Effect

The results of applying SIM to the three portions of the Avon Estuary yielded fractal dimensions from 1.06 to 1.38 (Figure 4.3). Correlation coefficients were high: the lowest R- value was 0.88 for -4 m within the upper and main channel of the Avon Estuary. A typical example from the Avon Estuary for a -2.5 m elevation, with a fractal dimension of 1.19 and a regression coefficient R of 0.93, is shown in Figure 4.4. The fractal dimensions within all three portions of the Avon Estuary vary with the elevation at which SIM was applied. The fractal dimension generally decreases with increasing elevation, up to an elevation around 1 m. A plateau can be noticed from 0 m to 3 m for the entire Avon and the upper portion. However the main channel presents a steady increase over this elevation range. It should be noted that the standard error of the slope also changes with elevation; between 0 and 3 m the error was consistently higher for all three sections, with the largest error range being in the main channel. The elevation range of increased error was also the range with the fewest islands

that were used in the analysis. Beyond the plateau from 0 m to 3 m, a noticeable spike in the fractal dimension was present in all three sections at 3.5 m.

In order to better interpret the similarities and differences between the three sections, each section of the Avon Estuary was compared to the average of all three sections for each elevation. The results are shown in Figure 4.3d. This type of representation shows that there are a number of areas where the difference between the three sections is minimal. It also shows where sections differ considerably; the greatest difference in fractal dimension between all three sections occurs around 3.5 m. The results were also represented as a central three point running mean in Figure 4.5. The three point running mean is calculated by averaging each elevation with the value before and after it. This smoothens the data and allows for general trends within the data to be better observable. This provides a better picture of the general trend in decreasing fractal dimension with an increase in elevation until around 0.5 m for all three sections. The overall patterns of the results are similar for all three sections, the main exception being the rate of decrease from -2 m to 0.5 m, and the increasing trend from 0.5 m to 2 m for the main channel compared to the other two sections (Figure 4.5).

4.6 Discussion

The results of the study show that the Avon Estuary is not a 3D isotropic, self-similar system, as the fractal analysis did not yield the same value for each elevation. This means that when applying fractal analysis methods to this kind of environment, the elevation at which it is performed should be specified, as it will impact the outcomes of the pattern analysis. This is probably the result of a number of different factors that

occur at certain elevations within the inter-tidal zone and dominate the formation of landforms over various elevation ranges.

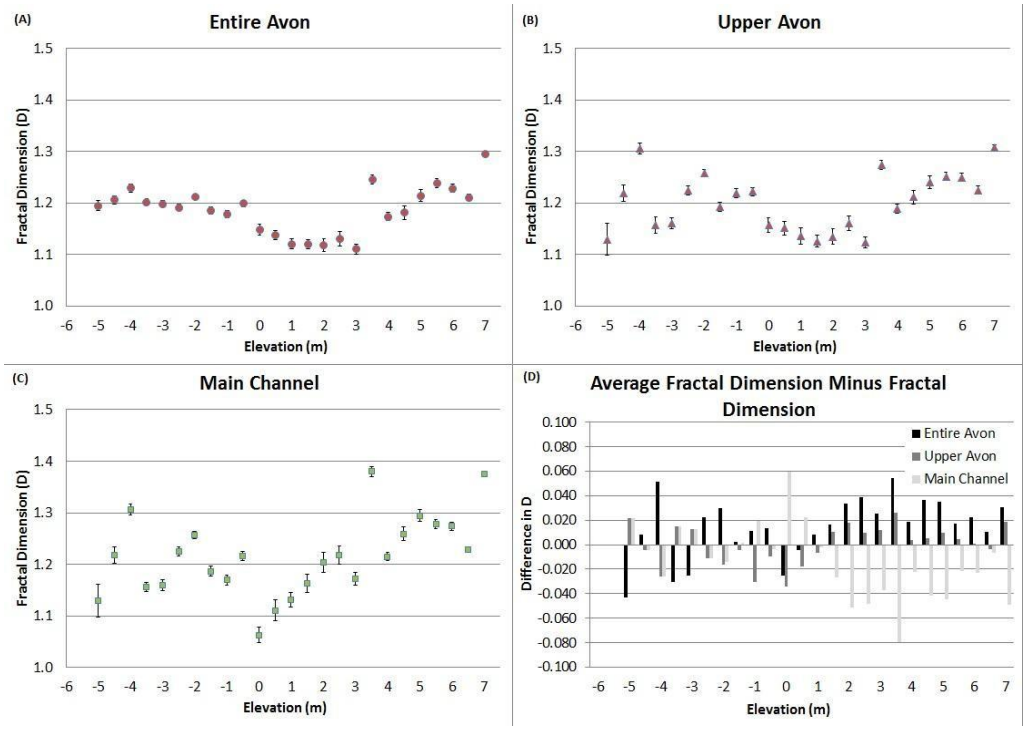

Figure 4.3: Results of the fractal analysis using Slit Island Method applied to a) the entire Avon Estuary, b) the upper portion and c) the main channel are shown above. The standard error of the slope is specified for each elevation. The difference between the fractal dimension values for each of the sections compared to the average fractal dimension found at each elevation is shown in the bottom right graph.

It is important to note that unlike other approaches to the characterization of irregular shapes, fractal analysis in general – and SIM in particular – also show that the same degree of irregularity is expressed on a range of scales. The results do not refer to the geometric properties of one individual feature (island) or another, but rather to the pattern that consists of the whole set of islands existing at the selected elevation. The power law form of the relationship between the area and the perimeter of all the

islands in the set is an unmistakable sign for the fact that the island contour lines in the set all correspond to the same degree of irregularity. The strong correlation that characterizes the power law relation reflects a high degree of confidence regarding the resulting pattern characterization.

Therefore, the results obtained with SIM do not depend on accidental, potentially irrelevant local morphological details: they reflect a characteristic of the pattern that is consistently found on many scales. In this study, the scale range for which the irregularity is characterized on each elevation is very wide, extending over several orders of magnitude (Figure 4.4).

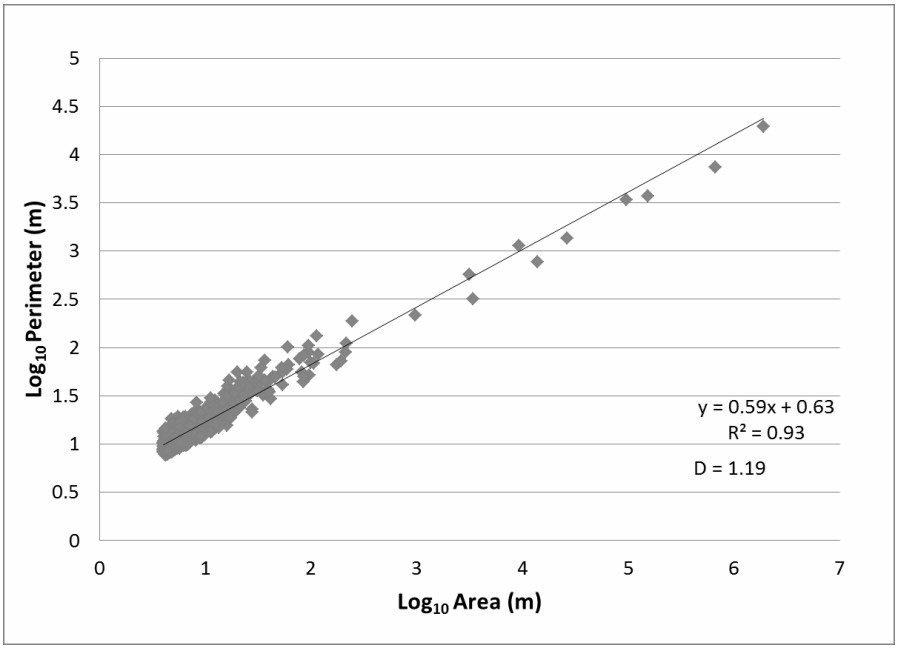

Figure 4.4 Example of results from fractal analysis using the Slit Island Method at an elevation of -2.5 m for the Entire Avon Estuary.

A higher value of the fractal dimension indicates an enhanced irregularity of the coastal pattern, i.e. a higher degree of spatial variability that characterizes the polygon

geometry of the set of islands defined by a certain elevation, on a wide range of scales. The SIM yielded fractal dimensions with a high correlation coefficient, often higher than 0.95.The results ranged from fractal dimensions of 1.0 to 1.38. This represents a wider range than the one reported by Schwimmer (2008), who, using another fractal analysis method (box- counting), found fractal dimensions of wave-dominated marshes in Delaware between 1.01 to 1.19, and dimensions of 1.27 to 1.28 for Allen Creek, a macro tidal salt marsh similar to those found within the Avon Estuary. The higher fractal dimensions found in the macro tidal environments are not surprising, as both the Avon Estuary and Allen Creek are dominated by tidal influences, more so than by wave action. This study confirms Schwimmer`s (2008) results regarding a higher spatial variability of tidal vs. wave dominated environments.

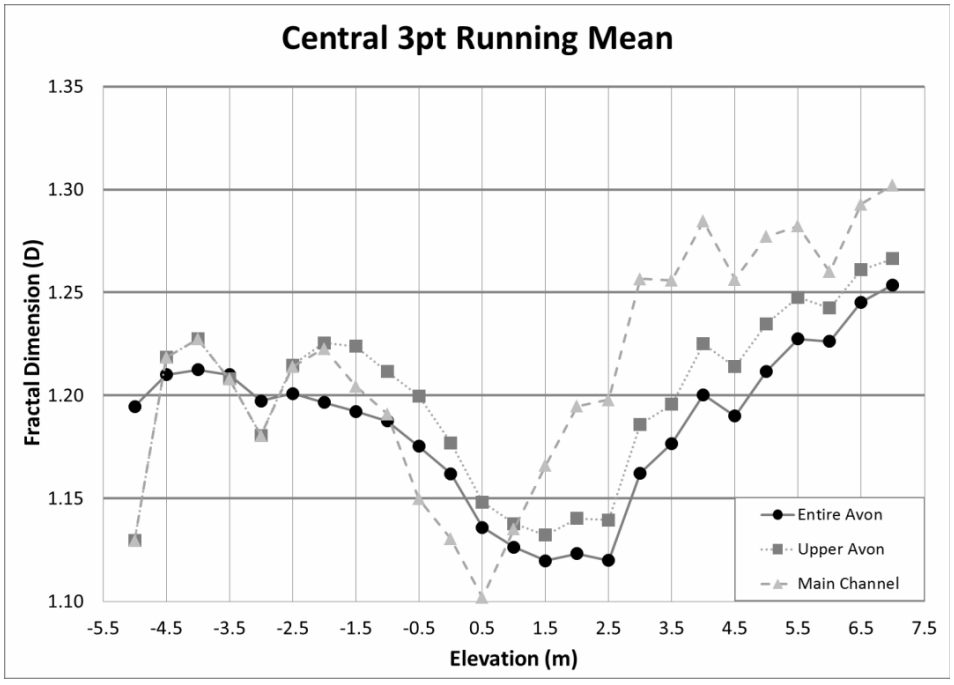

Figure 4.5: Central three point running mean of fractal dimension values for the main channel, upper Avon, and the entire Avon.

The three point running mean graph (Figure 4.5) suggests that while the Avon Estuary is not 3D self-similar, its different sections are similar over the studied elevation intervals. The changes in fractal dimension with elevation did not appear to be random. At the lowerelevations from 5 m to 2 m above datum (Figure 4.5) the results fluctuate around a dimension of 1.2. This environment is dominated by high flow velocity as tidal waters are constrained between intertidal bodies (Lambiase, 1980) and the redistribution of sediment is continually contributing to the formation of inter-tidal sand bars. The tidal bars themselves are dominated by sand waves (wave length 30-75 m), mega-ripples (wave lengths 2-8 m) resulting in the formation of islands at lower elevations (van Proosdij, 2007) (Table 1).

Table 4.1: Summary of geomorphic zones determined through the Slit Island Method. All elevations are expressed relative to tidal elevations converted to CGVD28 datum.

Elev. zone	D range	Dominant Process	Intertidal Feature
-5 to -2 m	~ 1.2	Bedform development - sand	Sandwaves with megaripples
-2 to -1 m	~1.18	Bidirectional sediment transport	Bidirectional ripples with veneer of Fines
-0.5 to 1.5m	1.17 – 1.13	Vertical accretion with bank erosion	Accreting mudflat
1.5 – 2.5m	~1.13	Vertical accretion with thalweg erosion	Establishment of mudflat tidal channel Network
2.5 – 4 m	1.13-1.2	Vertical accretion & sediment trapping by patches of vegetation	Patches of *spartina alterniflora* on accreting mudflats
4 – 7.5 m	1.12 – 1.25	Substrate stabilization by vegetation	Continuous coverage of *Spartina sp.*

These islands are often only delineating parts of the sand wave or mega-ripples within a tidal bar (Figure 4.8a). Mean sediment grain size has been reported lie between 125 to

250 μm (Pelletier and McMullen, 1972; Lambiase, 1980) in this area. Between -2 to -1 m above datum, bidirectional ripples with a thin veneer of fines occur with a dimension of 1.8 (Figure 4.8b). D values decrease between -0.5 to 1.5 as vertical deposition of medium to coarse silt dominates on developing mudflats. These flats are constrained by erosion at the edges of the bank as currents are constrained between the growing intertidal bodies (Lambiase, 1980) (Figure 4.8c). The larger tidal bars are elongated due to tidal flow and the directional dependence on flow has led to a smoother formation (Dalrymple *et al.*, 1990), lowering the D value. Dimension remains relatively constant at approximately 1.13 as channel networks begin to be more defined within the mudflat surfaces (Figure 4.8d). In addition, the transition between 1.5 to 2.5 m CGVD28 (Figures 4.5 & 4.6) appears to represent a shift to a depositional environment with increasing fines. Sediments in this region have a mean of 23-30 μm with well sorted, fine silts (68%) with a substantial clay fraction (23%) (Daborn et al., 2003). Above 3.0 m above datum, vegetation begins to be established with isolated patches (Figure 4.8e) which then coalesce into continuous vegetation coverage after 4.0 m. This results in an increase in D values from 1.2 to 1.25.

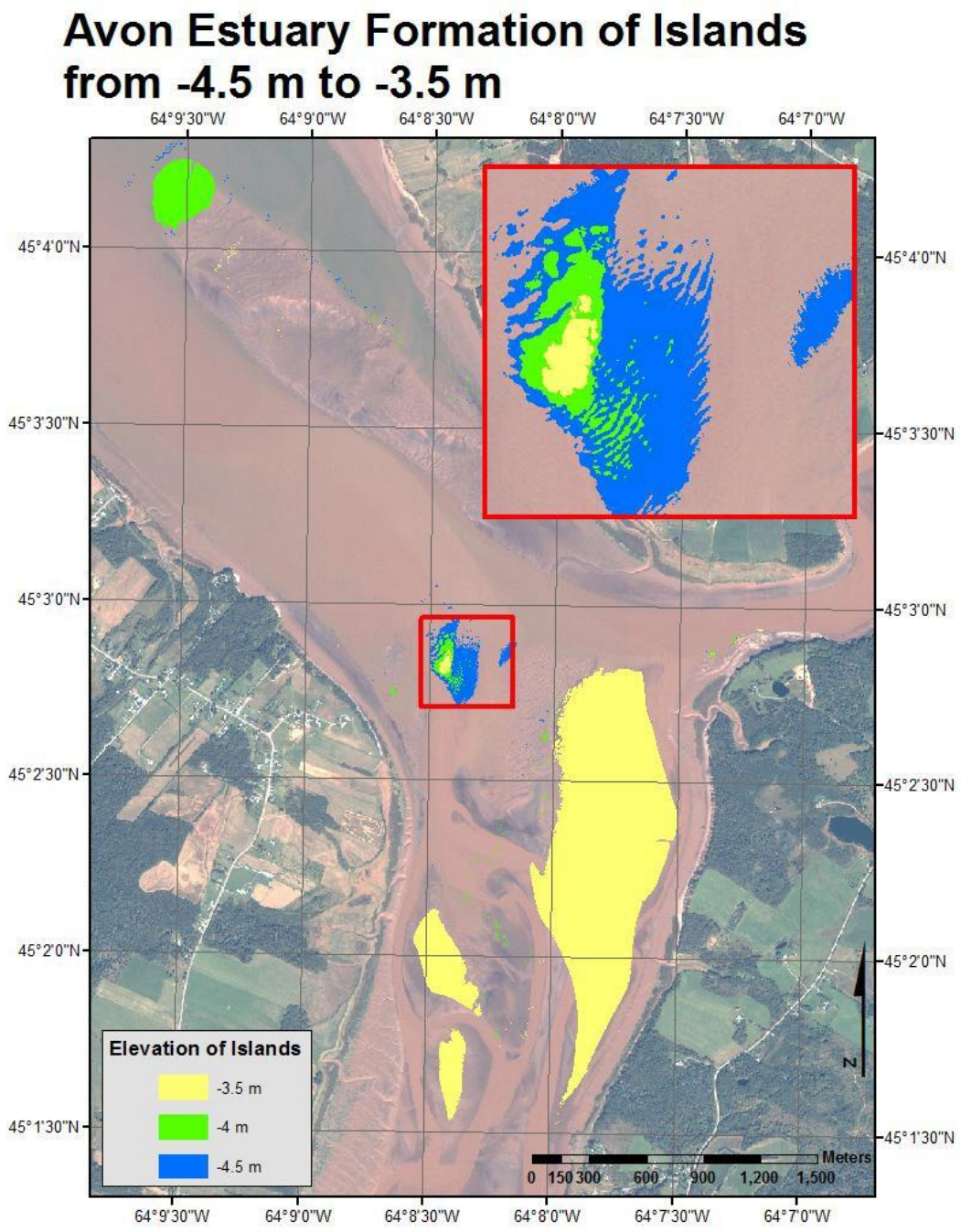

Figure 4.6 A 4 m resolution Ikonos Image from 2007 of the Avon Estuary along with the islands generated using the SIM for elevations between -4.5 m and -3.5 m. At -4.5 m and -4 m above datum the islands are dominated by the formation of sand waves and mega-ripples. At -3.5 m above datum larger more permanent tidal bars start to form.

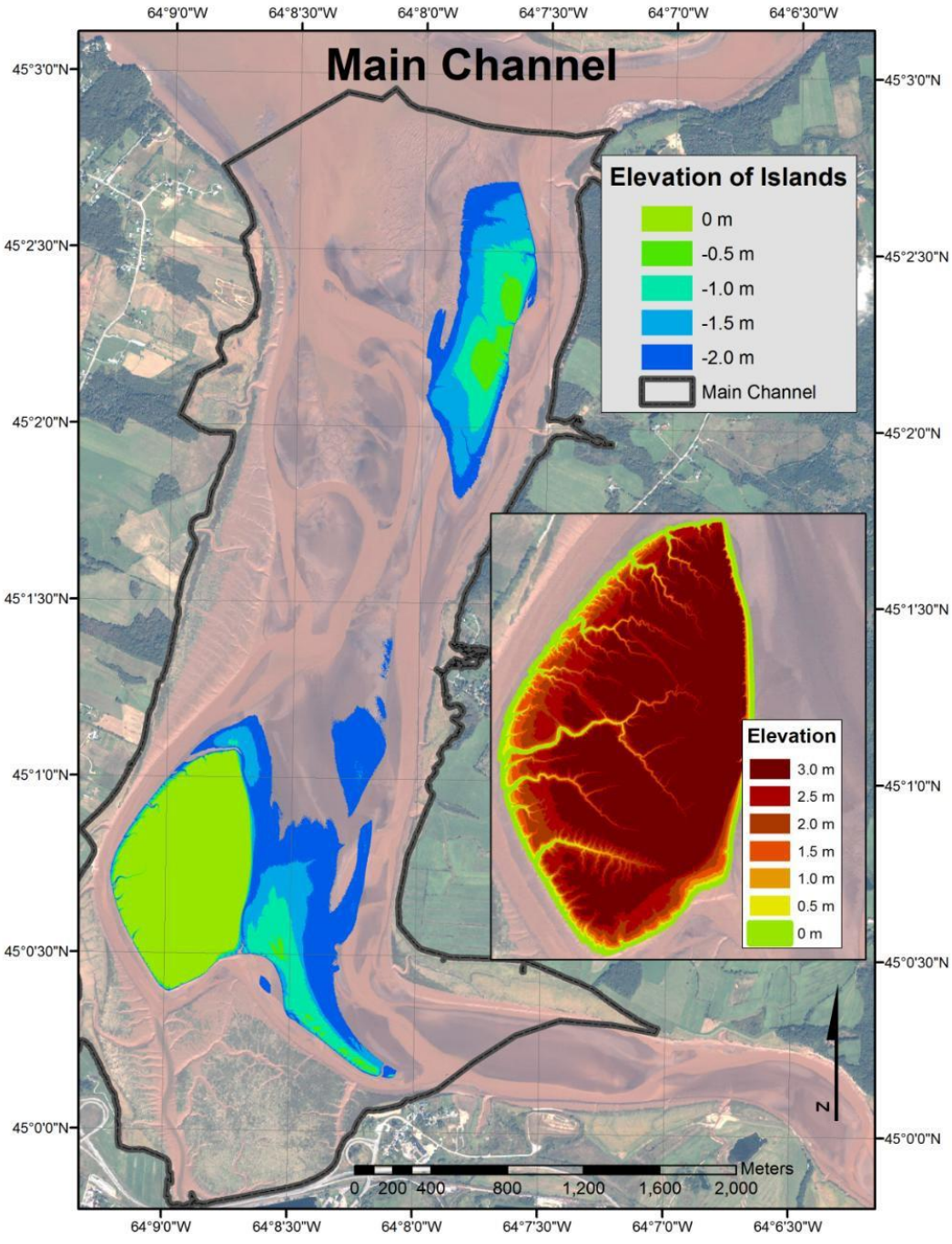

Figure 4.7: A 4 m resolution Ikonos Image from 2007 of the Avon Estuary along with the islands generated using the SIM for an elevation of -2.0 m to 3 m. The figure shows the presence of more direction dependent islands and the formation of channel networks at higher elevations. The presence of vegetation at 4 m above datum is evident in a 2007.

Ikonos image from the same time period of the data collection (Figure 4.7). Vegetation becomes one of the dominating factors in sedimentation within this elevation range as it alters the velocity of flow, enabling suspended sediment to settle (Friedrichs and Perry, 2001). Once vegetation, notably *Spartina alterniflora* becomes established, the tidal creek boundaries become more stabilized, preserving the shape of the tidal creek network (Allen, 2000). The highest fractal dimensions are found within the mid to high marsh, which is a depositional environment.

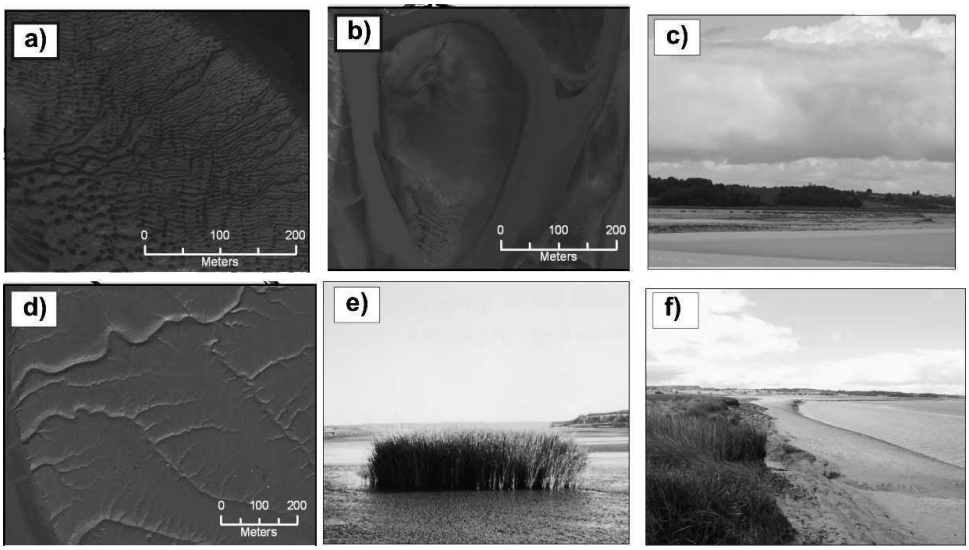

Figure 4.8: Dominant intertidal features identified by zone using Ikonos 2007 panchromatic imagery and field observations. Features are identified as (a) sandwaves with megaripples; (b) bidirectional ripples with a thin veneer of fines; (c) rapidly accreting mudflat with some vegetation colonization and bank erosion (photo taken in September2006); (d) intricate mudflat channel network; (e) photo from September 2007 depicting Spartina alterniflora colony; and (f) complete Spartina coverage with bank erosion.

This is in contrast to Schwimmer (2008) where more erosional environments where found to have higher fractal dimension. This study shows that deposition in the presence of vegetation can produce patterns which are more intricate than in an environment lacking vegetation. These island patterns consistently preserve their degree of irregularity on scale ranges that span several orders of magnitude. In other

words, the depositional features and the spatial pattern of vegetation growth on different scales emphasize the same variability. This indicates that we are not witnessing just a vegetation-affected depositional process, but rather a set of interacting processes involving feedback loops on many scales. The high marsh within the Avon Estuary is also being affected by dykes that were created to reclaim farmland and limit the extent of the Estuary during high tides: the results of this study suggest that a comparative analysis based on the same methodology and also involving an area not affected by such anthropogenic influences may reveal the implications of dykes for pattern formation in a tidal environment.

4.7 Conclusion

Following the application of SIM to the Avon Estuary over a multitude of elevations it was determined that coastline patterns – produced by the intersection between the landscape and horizontal planes – are elevation dependent. The change in fractal dimension with elevation did not appear to be random; the pattern for all three studied sections of the Avon Estuary followed the same general trends. In addition to quantitatively assessing self- affinity within an inner tidal zone, the analysis also pointed to links between form and processes: changes in fractal dimension correspond to ranges of dominant processes, some of which have been subject to anthropogenic influences. Higher fractal dimensions are generally associated with depositional processes and stabilization by vegetation whereas lower D values are associated largely with erosional processes and coarser sediments. Further studies are required on similar environments, including those that have not been affected by anthropogenic factors, to improve our understanding of the links between form and process.

Chapter 5 Assessing the Effects of Interpolation Methods Used to Produce DEM on the Scaling Analysis.

This chapter investigated the effects that interpolation algorithms have on the creation of DEM from LiDAR datasets and their impact on scaling analysis. An error analysis was performed on three commonly used gridding algorithms used within GIS: spline, natural neighbour and IDW. In addition to performing an error analysis on the three DEM, the SIM was applied to each of the derived DEM and a comparison of the resulting fractal dimension was performed to see if the interpolation method will have an effect on the fractal analysis.

5.1 DEM Interpolation Methods

A DEM is a data file containing an array of elevation data. The information within a DEM can come from a number of data sources such as ground based surveyed points, contours, interferometry, radar, photogrammetry and LiDAR. Often, the DEM is at a finer scale than the data or the datum is not evenly distributed, resulting in areas within the DEM not having known points associated. How elevation data are assigned to areas without known points is important as it may affect the overall accuracy of the DEM and potentially any analysis that is performed on it. The act of estimating elevation for areas without elevation data **is** a form of interpolation. The areas of unknown elevation are assigned a value based on the known points around it. There are a number of commonly used interpolation algorithms such as Inversed Distance Weighting (IDW), natural neighbour, spline, and kriging (Lo, Yeung, 2002). Each of these methods has advantages and disadvantages to them and some work better in certain circumstances

than others. Interpolation methods that pass the generated surface through all known points are called exact interpolators whereas those that do not pass exactly through the known points are called inexact interpolators (Apaydin, et al, 2004). Interpolation methods applied to LiDAR data sets have been previously assessed for forested areas; it was found that the natural neighbour method produces lower errors compared to spline and IDW (Bater, Coops, 2009). This chapter presents the assessment of the error associated with natural neighbor, spline and IDW when applied to a LiDAR dataset over the Avon Estuary.

5.1.1 Spline

The spline is an exact interpolation method as its generated surface will pass through all known points. The spline method applies a mathematical function in order to minimize overall surface curvature when estimating elevation values. The surface generated using spline is a combination of element surfaces defined by a basis function. Basis functions can be polynomial, logarithmic or radial. In the case of ArcGIS, when applying spline a radial basis function is used. Essentially Spline can be thought of as applying a surface to known elevation points and minimizing the curvature between the points in order to produce a surface that maintains the known elevations and limits the peaks and valleys of the surface. The ability to represent peaks and valleys where there are no known points sets it apart from both IDW and natural neighbour, which are limited to the elevation range of neighbouring points. This can also lead to interpolated surfaces using spline to have over-shooting or under-shooting elevations within the DEM. (Ref)

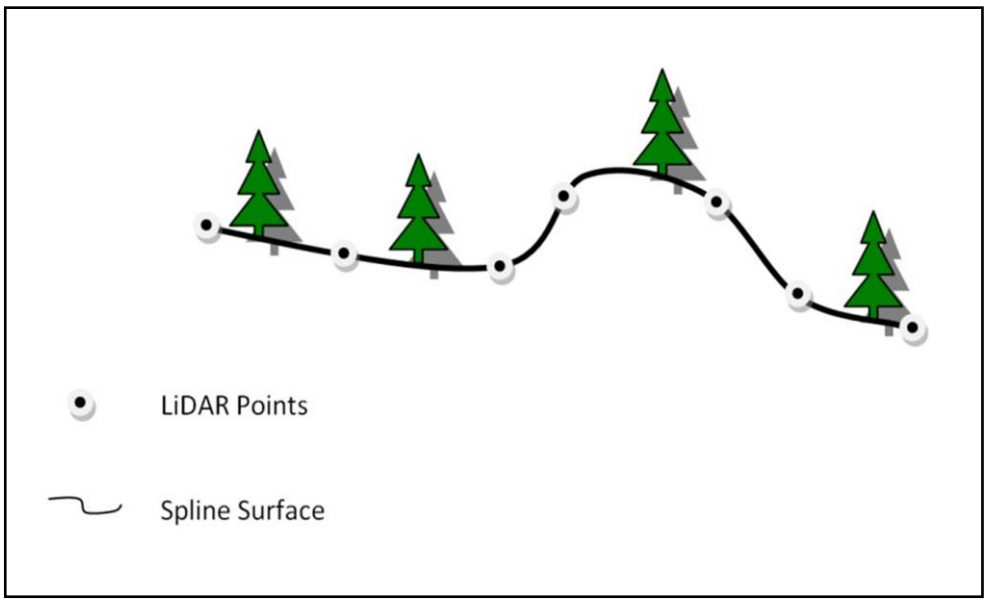

Figure 5.1 Representation of a spline interpolated surface passed through LiDAR ground returns. It results in a smooth surface with some peaks and valleys which are restrained by the LiDAR points.

Within ArcGIS there are two variations of spline that can be used as an interpolation method, which are spline with tension and regularized spline. Regularized spline has been shown above. The spline with tension creates a DEM that is not as smooth as its counterpart as it assigns a weight to limit the amount of variation from the known points. Due to the lack of LiDAR returns within the channel networks where water was present (chapter 3), the regularized spline was chosen as it results in a greater range in surface values that can be higher than the known points around it if the surface is trending upwards or downwards. Regularized spline is prone to higher levels of error when there are artifacts within the data (Bater and Coops., 2009) as the interpolation method will force the DEM to pass its surface through these artifacts. LiDAR data that are not properly classified can often return low vegetation as the ground, causing the DEM to higher elevations then actual elevations on the surface.

5.1.2 Inversed Distance Weighting

IDW is similar to spline as it is also an exact interpolator, and it too is prone to increased error when artifacts are present in the data as the surface is forced to pass through each known point. The quality of surfaces generated using IDW is dependent on the accuracy, density, and the distribution of input points, as gaps in the data will result in flattening of the surface (Lo, Yeung, 2002). The weights used in IDW are inversely related to the squared distance between the known points and the unknown sample location. Essentially, the estimated elevations of unknown locations are more dependent on the elevations from points closer than those further away. The elevations are a function of an average of weighted distance limited by the highest and lowest elevations. If the extremes within the topography have not been surveyed then IDW cannot generate ridges or valleys (Waston, Philip 1985).

In areas where there is only one surveyed point within the search radius of the IDW command the resulting DEM will have what is commonly known as bulls eyes., In the case of IDW, a bulls eye refers to a ring around the point of decreasing or increasing elevation, as there is only one point to base the surface off of for that general location.

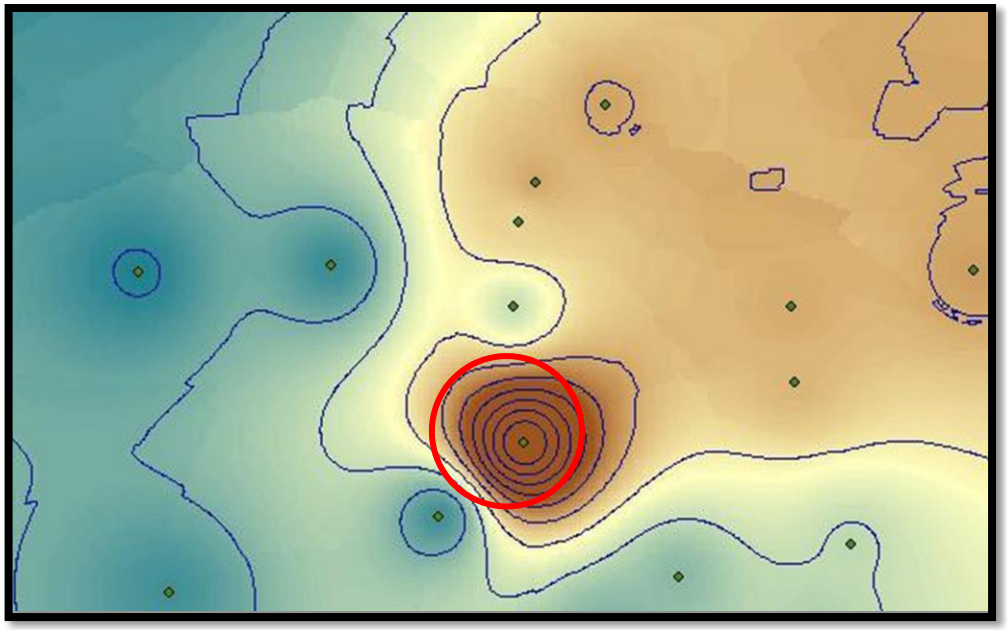

Figure 5.2 Representation of an IDW interpolated surface showing the bull's eye effect caused by applying IDW to areas of low point density shown in the red circle.

5.1.3 Natural Neighbour

Natural neighbour is a local interpolator, as it only considers a subset of the known points for any given location within the DEM, and the areas that have known points on the surface will pass exactly through each point's elevation. The elevations that are interpolated using natural neighbour have weights that are assigned based on generating Thiessen polygons around all known points and then applying a new set of Thiessen polygons around the un-sampled locations. The weights for the un-sampled locations are based on the area of overlap between the un-sampled location Thiessen polygons and the Thiessen polygons derived from known points (ESRI, 2010).

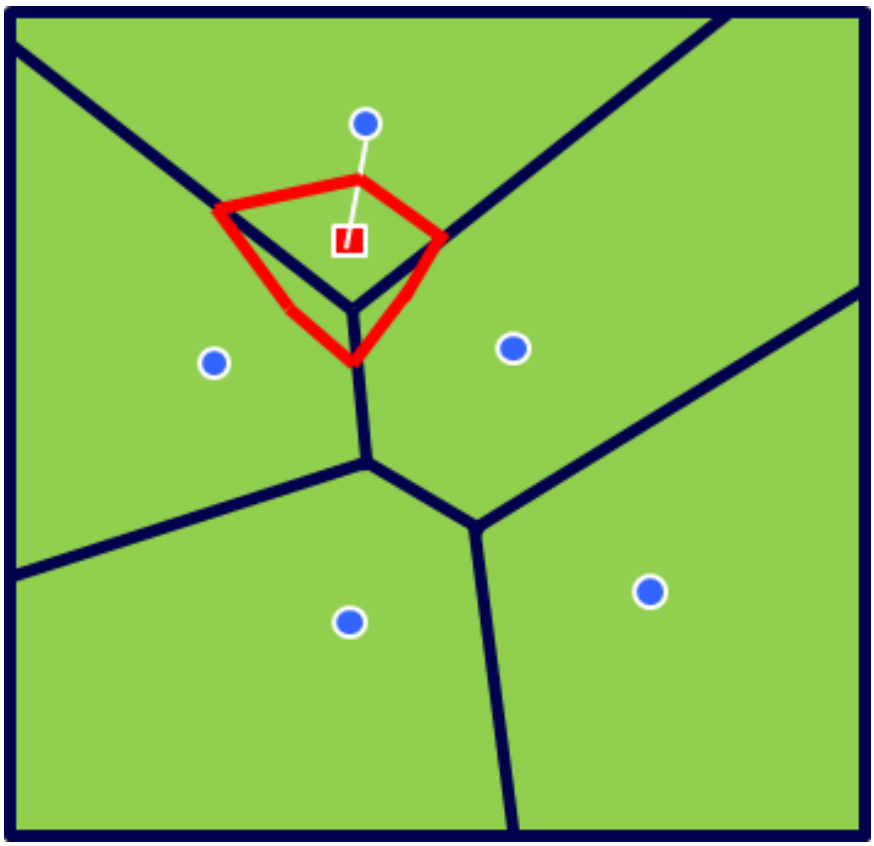

Figure 5.3 The weights of the un-sampled location are derived from the area of overlap of the Thiessen polygons generated from the known points shown in black and the Thiessen polygon of the un-sampled location shown in red.

Since the un-sampled location is derived from weights of known points, the elevation cannot positively or negatively exceed their elevations,resulting in the method's inability to generate peaks or valleys where there are no known points along those features (ESRI, 2010). The performance of natural neighbour is not dependent on how the data are distributed but rather on how dense the data are (Watson, 1992). Natural neighbor would be an ideal interpolation method for LiDAR surveys over surfaces such as dense canopy cover where pools of water may cause gaps within the data resulting in the ground returns being irregularly distributed.

5.2. Study Area

Given the large amount of LiDAR points that were collected over the Avon Estuary and the lengthy processing time of the interpolating the surfaces from the LiDAR points, a sub section around the Windsor causeway was chosen to evaluate the effects that interpolation methods have on the SIM.

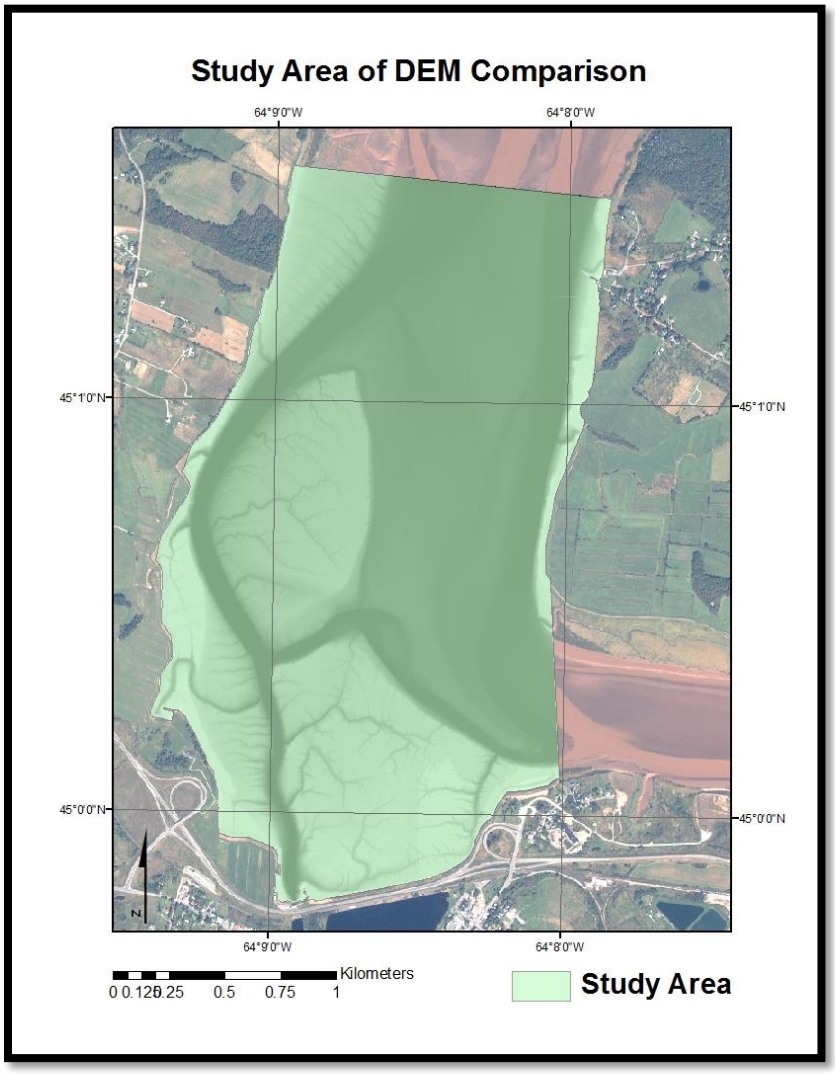

Figure 5.4 The boundary of the three DEM that were generated using IDW, spline and natural neighbour interpolation methods is shown in green. The study area encompasses the Windsor mudflats that formed in front of the Windsor causeway.

The LiDAR points were distributed throughout the study area. The distance between the points ranged from approximately 0.4 m to 1.2 m (Figure 5.5). The DEM was generated at 1 m grid spacing as the majority of points were near or below 1 m spacing. In areas of standing water the point spacing was as high as 1.8 m. The survey was collected during low tide, to minimize the presence of water within the survey, allowing for more evenly distributed data points with fewer gaps.

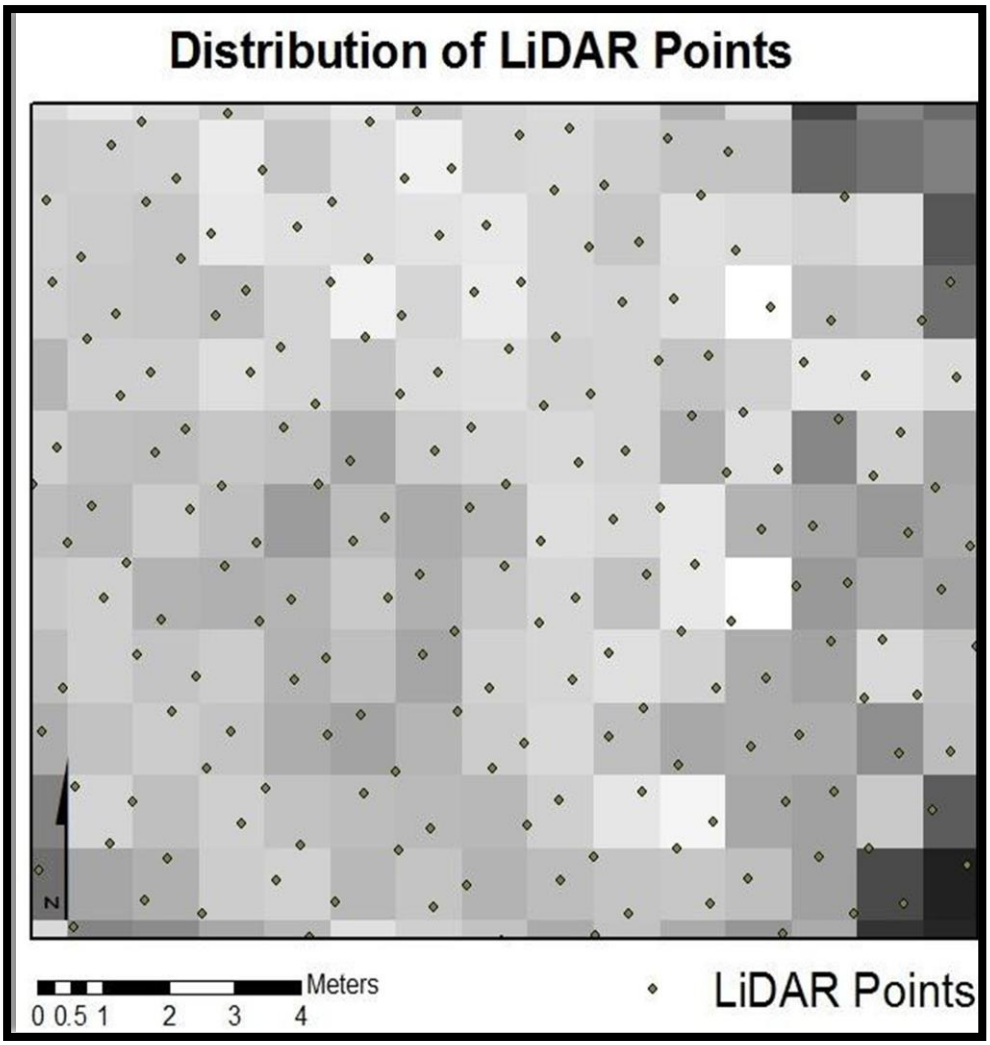

Figure 5.5 Distribution of LiDAR points from a subsection of the study area near the Windsor causeway.

5.3 DEM Generation

5.3.1 Data Preparation

The raw LiDAR data were processed using Optech proprietary software Realm 3.2. Realm is used to merge the IMU data, the corrected GPS data and the range data in order to generate Log ASCII Standard (LAS) files which contain the combined information from the LiDAR systems. The LAS file is then classified in Terra Scan, which is an add-on to Bentley Micro Station, in order to classify out only the ground returns. The ground returns were then exported into a text file containing the latitude, longitude, elevation and intensity for each point. The LAS files were separated into 1 km tiles as there were too many points for the software to handle all at once due to computer system limitations.

The resulting ground return points were then converted to a shape file, within ArcGIS, and used as the input data for the generation of the DEMs. There were 14 tiles that were used to cover the Windsor mudflats which were the study area of the DEM comparison. The tiles were set to 1040 m by 1040 m in order to have a 20 m overlap between adjacent tiles so that a seamless mosaic could be produced from the interpolated tiles.

5.3.2 Settings Used in the Interpolation

The three DEMs which were used for the comparison were all generated using ESRI ArcGIS 9.3 software. The output cell size was set to 1 m for all of the interpolation methods. The input features were the point shape files that were generated from the ground returns of the April 3rd 2007, LiDAR survey of the Avon Estuary For spline the regularized option was chosen with a weight of 0.1 and the number of points was set at 10. For IDW the search radius was set to 5 m.

5.4 SIM applied to DEMs

The SIM was applied to the DEMs by contouring at 0.5 m intervals. The contouring command within 3D analyst, an extension of ArcGIS 9.3, was used in this process with a z factor of 1 as the X Y Z units are all using meters as measurement, so no unit conversion was required. The contours were then clipped to the study area that was limited to the tidal extent of the Avon Estuary around the Windsor mudflats (Figure 5.4). The resulting contours for all three methods show differences within each of the elevation ranges (Figure 5.6). The contours which were derived using spline are in line with those from natural neighbor, resulting in only the minor differences being visible (Figure5.6). The areas where spline has the greatest differences from natural neighbour and IDW appear to be the highest points within the local areas of the DEMs and is probably due to the fact that the spline algorithm is not limited to the highest elevation. Since spline is not limited to the known elevations it can interpolate local trends within the data and represent peaks and valleys resulting in the modeling of higher amounts of islands then other interpolated surface (Figure 5.6).

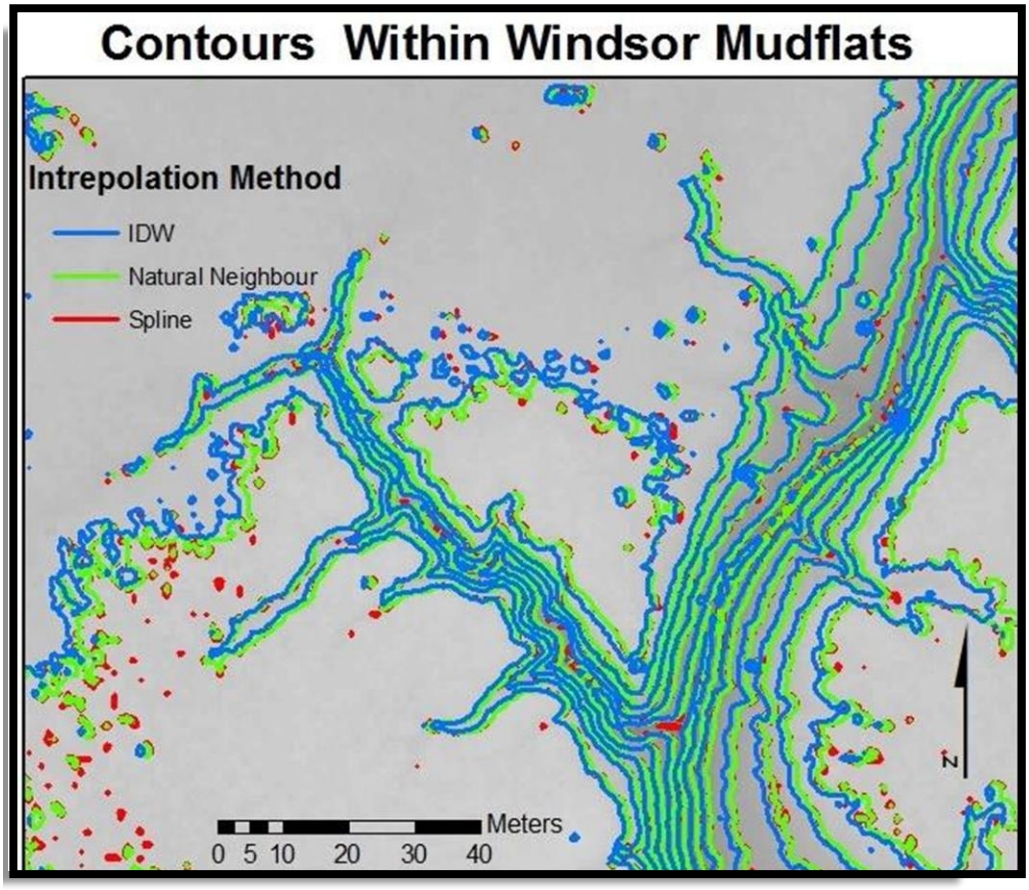

Figure 5.6 Contours within the Windsor mudflats generated from DEMs interpolated using IDW, natural neighbour and spline.

The corresponding closed contours for each of the interpolation methods were then converted to polygons and only islands that were greater than 4 m in area were considered. This was done to minimize the impacts of small errors within the DEM that would result in small islands artificially forming. The numbers of islands generated for almost all of the elevations were different for each of the DEMs. The DEM that was produced using spline had the largest amount of islands (3723) compared to 2670 islands for natural neighbour and 2800 for IDW. Differences in the number of islands that were generated shows that there are elevation differences among the DEMs as they did not produce the same amount of islands for each elevation.

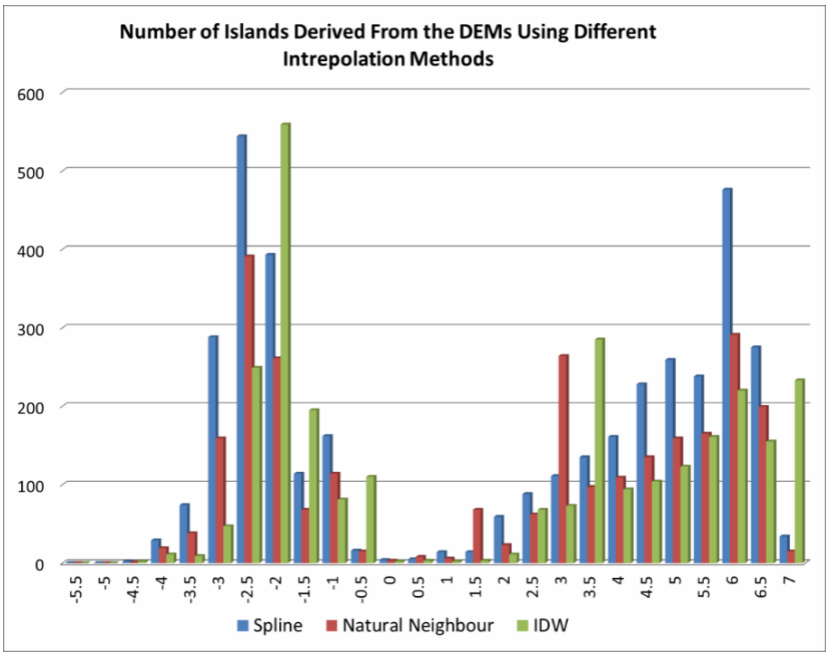

Figure 5.7 Comparison of the total number of islands generated for each elevation using DEMs interpolated by spline, natural neighbour and IDW.

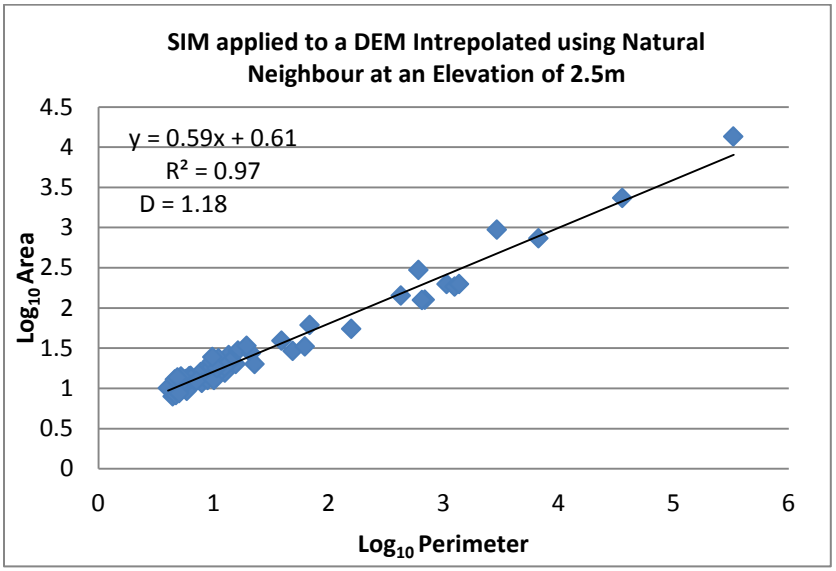

Figure 5.8 Example of an output from the analysis of SIM applied to an elevation of 2.5 m from islands generated using a natural neighbour DEM where D represents the fractal dimension.

The process of evaluating closed contours for each chosen elevation simulates the passing of a plane through the DEMs. The resulting islands were compared by graphing the $\log_{10}$ of the area to the $\log_{10}$ of their perimeter. A best fit line was applied and the fractal dimension was calculated as two times the slope. An example of this is shown in figure 5.8. A more in depth review of the SIM method is presented in chapter two.

5.5 Results

The difference in the resulting fractal dimensions from applying the SIM to the three DEMs is shown in figure 5.9. Some elevations did not have enough islands for analysis, which limited the direct comparison of the three interpolated methods over the entire elevation range. Unlike other fractal methods, such as the divider method, which uses a set of points which are equally spaced along the X Y axes, the SIM is based on measured islands. This can result in the measured islands being clustered on different scale ranges, which can influence the regression process and thus the resulting exponent. The appropriate number of points depends on the distribution of the points in scale space. For this study a minimum number of five islands distributed over at least one order of magnitude was chosen as the minimum distribution range when applying the SIM. There were no islands for all three of the interpolated surfaces below an elevation of -4 m, as lower elevations were within channel networks extending outside of the study area and thus would not produce closed contours. Contours that did not close were discarded when applying the SIM. In addition there were not enough islands at an elevation of 0 m for all three DEMs. The IDW interpolated surface had the largest gap in elevations without enough islands, which ranged from 0 m to 1.5 m. Generally,

the resulting fractal dimensions from each of the interpolated surfaces followed the same trend as each other with a few exceptions; at 3.5 m IDW has a relatively low fractal dimension of 1.09 where the fractal dimension derived from spline is 1.52 and natural neighbour 1.428. At -2.5 m the fractal dimension for IDW is moderately higher at 1.48 compared to the others which are around 1.3.

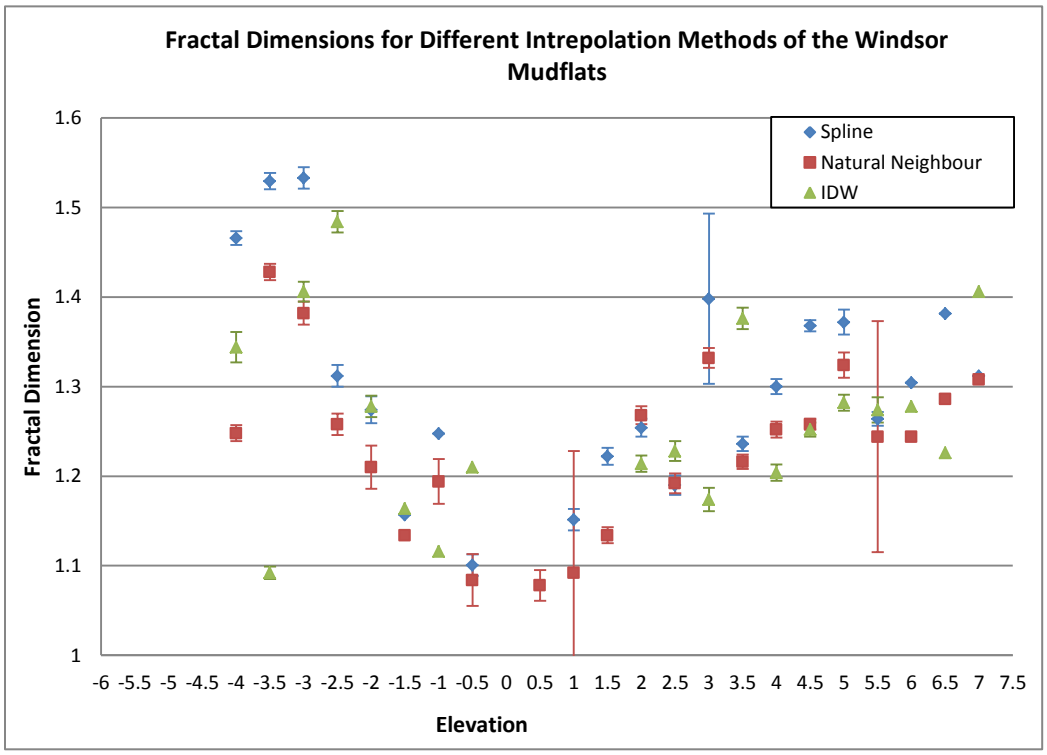

Figure 5.9 Fractal Dimension for different interpolation methods of the Windsor mudflats. SIM was applied to three DEMs interpolated using spline, natural neighbour and IDW. The error bars were calculated as the standard error of the slope of a best fit line passed through the area vs. perimeter for a log10 log10 graph. The elevation contours were relative to CGVD28 chart datum

The spline DEM on average produced the highest fractal dimension for each elevation, having the highest value for 12 out of the 22 elevations presented. When the fractal dimensions from all three interpolation methods were averaged, the fractal dimensions

derived from using the spline DEM had higher than average values for 16 out of 22 elevations (Figure 5.10). The greatest difference in the fractal dimension for spline was 0.17, and occurred at an elevation of -3.5 m.

Natural neighbour DEM, on average, produced the lowest fractal dimension with 13 out of the 22 elevations having the lowest values. The maximum difference in fractal dimension from the average for natural neighbour was 0.10. However the fractal dimension for natural neighbour presented the lowest differences between average values and natural neighbour values. There were only three elevations that produced a difference in the fractal dimension greater than 0.05 compared to the average at each elevation for natural neighbour. This was lower than both the spline and IDW, as spline had 7 and IDW 8 elevations with fractal dimension greater than 0.05 compared to the average.

Like spline, the numbers of fractal dimensions for IDW compared to the average fractal dimensions were higher than natural neighbour. IDW had 3 elevations that exceeded a difference of 0.1 and at -2.5 m the difference was 0.13 compared to the average fractal dimension for that elevation. However IDW did have the lowest average standard error associated with it. The standard error of the slope for IDW had an average error of 0.014 compared to 0.018 for spline and 0.027 for natural neighbour. Lastly, IDW had five elevation ranges that were dropped as there were not enough islands for meaningful analysis.

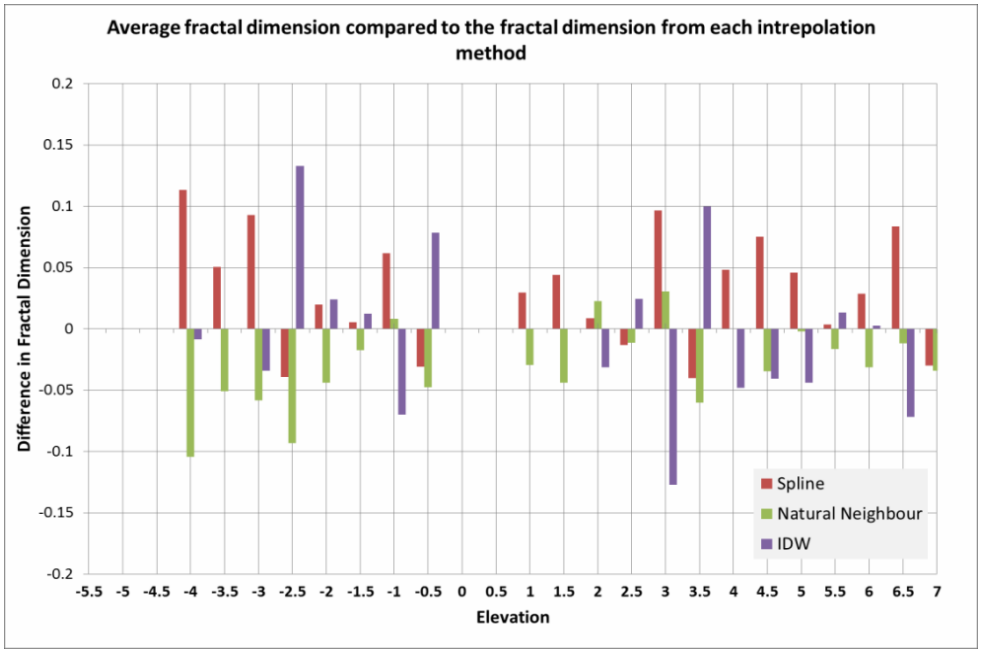

Figure 5.10 The average fractal dimension was calculated at each elevation using the SIM applied to spline, natural neighbour and IDW derived DEMs. The fractal dimension using each interpolation method was then subtracted by the average fractal dimension and the difference was plotted.

	Spline				Natural Neighbor				IDW				
Elevat	#	D	error	R^2	#	D	error	R^2	# Islands	D	error	R^2	Range (D)
-5.5	0				0				0				
-5	0				0				0				
-4.5	2				1				2				
-4	29	1.47	0.06	0.83	19	1.25	0.05	0.90	11	1.34	0.05	0.96	0.22
-3.5	74	1.53	0.03	0.91	38	1.43	0.04	0.88	9				0.10
-3	288	1.53	0.02	0.90	159	1.38	0.02	0.91	47	1.41	0.04	0.87	0.15
-2.5	544	1.31	0.01	0.92	391	1.26	0.01	0.94	249	1.48	0.02	0.89	0.23
-2	393	1.27	0.01	0.93	261	1.21	0.01	0.94	559	1.28	0.01	0.93	0.07
-1.5	114	1.16	0.01	0.96	68	1.13	0.01	0.97	195	1.16	0.01	0.93	0.03
-1	162	1.25	0.01	0.94	114	1.19	0.01	0.96	81	1.12	0.01	0.97	0.13
-0.5	16	1.10	0.02	0.99	15	1.08	0.02	0.98	110	1.21	0.01	0.96	0.11
0	4				3				2				
0.5	5				8	1.08	0.03	0.99	3				
1	14	1.15	0.01	1.00	6	1.09	0.03	0.99	2				0.06
1.5	14	1.22	0.02	0.99	68	1.13	0.01	0.97	3				0.09
2	59	1.25	0.02	0.97	23	1.27	0.02	0.99	11	1.21	0.02	0.99	0.05
2.5	88	1.19	0.01	0.97	62	1.19	0.14	0.97	68	1.23	0.02	0.98	0.04
3	111	1.40	0.01	0.93	264	1.33	0.01	0.95	73	1.17	0.01	0.97	0.22
3.5	135	1.24	0.01	0.97	97	1.22	0.01	0.97	285	1.38	0.01	0.95	0.16
4	161	1.30	0.01	0.95	109	1.25	0.01	0.97	94	1.20	0.01	0.97	0.10
4.5	228	1.37	0.10	0.96	135	1.26	0.01	0.96	104	1.25	0.01	0.96	0.09
5	259	1.37	0.01	0.97	159	1.32	0.01	0.98	123	1.28	0.01	0.96	0.09
5.5	238	1.26	0.01	0.96	165	1.24	0.01	0.97	161	1.27	0.01	0.97	0.03
6	476	1.30	0.01	0.96	291	1.24	0.01	0.97	220	1.28	0.01	0.96	0.06
6.5	275	1.38	0.01	0.90	199	1.29	0.01	0.92	155	1.23	0.01	0.97	0.16
7	34	1.31	0.01	1.00	15	1.31	0.13	1.00	233	1.41	0.01	0.92	0.10
Maxium D Value					Lowest D Value							averag	0.11

Figure 5.11 Results from applying the SIM to three DEM using Spline, Natural Neighbor and IDW. The D value represents the fractal dimension. The values highlighted in red show the maximum D value for that elevation and the values shaded in blue show the lowest D value. The range provides the difference between the highest and lowest values

5.6 Discussion

When applying the SIM to a DEM the interpolation method does influence the results of the scaling analysis, (Figure 5.9). If there was no influence then all three interpolation methods would have yielded the same fractal dimension for each elevation, which was not the case. However, the overall pattern in the change of fractal dimension with elevation remains similar for all three interpolation methods. There were a few elevations where the difference in the fractal dimension was higher than 0.2**:** at -4 m, -2.5 m and 3 m. Since the fractal dimension is influenced by the interpolation method then it is important to note how the DEM was generated when conducting the SIM on this type of data source. The study also showed that the type of interpolation method influenced the number of islands that was generated. The DEM produced using spline, which allowed over overshooting and undershooting of the modeled surface, resulted in higher amounts of smaller islands being modeled than from natural neighbor or IDW. It is important to note that the fractal dimension using SIM is based on the islands spanning over a wide range of scales which limits the influence of the clustering of smaller islands.

This study did not determine which interpolation method is best for scaling analysis; however it did show that the interpolation method does influence the D value. It is also

important to note that for spline and IDW the settings used in the interpolation could also have an effect on the results. The setting controls how many points are considered. Changes in these settings are expected to affect the shape of the DEM which ultimately could affect the shape and the number of islands produced using the SIM.

The reliability of the interpolation methods is dependent on the data source, accuracy and spacing. It is recommended for future work that an error analysis be performed on the 3 DEMs for the Windsor mudflats to determine the appropriate DEM surface for analysis.

Chapter 6 Slit Island Method Applied to Sub-Sections of the Avon Estuary

In chapter four the fractal dimension was derived from three sections of the Avon Estuary: the entire estuary, one without the Kennetcook River but with the St. Croix River and, lastly, one without either of the tidal rivers. The self-similarity of the Avon Estuary was assessed, using the SIM, and differences were noted among subsections of the Avon Estuary compared to whole. The previous study (chapter 4) showed that the presence of tidal rivers within the analysis altered the fractal dimension and that a more refined look at the different subsections was warranted.

This chapter investigated the tidal rivers to see if they have different fractal dimensions compared to the main channel. The SIM was applied to five sections of the Avon Estuary: the upper, middle, and lower portions of the main channel along with the two tidal rivers the Kennetcook and lastly the St. Croix River (Figure 6.1). Unlike the previous study, presented in chapter four, the subsections do not have any overlapping boundaries (Fig. 4.1), allowing the fractal dimension to be linked to the processes governing the formation of islands in that region without being influenced from other regions. The fractal dimensions were derived at half meter intervals within the intertidal zone from low tide to highest high water large tide (HHWLT) level (~7.5 m above CGVD28 vertical datum at Hantsport – Canadian Hydrographic Service Chart 4140 1969). The tidal range of the Avon Estuary is from -5 m to 7.5 m above geodetic datum (CGVD28). For each of the five sections studied, the fractal dimensions were compared and links were made to the processes that dominated the formations of islands at each of the elevation ranges. In addition, the fractal dimensions from the five

sections were also compared to each other though there were a number of elevation ranges which could not be compared as there was not a sufficient number of islands or the islands did not range over at least 1 order of magnitude.

6.1 Study Areas

As mentioned above the Avon Estuary was divided up into five different sub-sections, with no overlap between the sections, so they could be compared independently of each other. Both of the major tidal rivers, the Kennetcook and the St. Croix River were designated as separate sections. This allowed for a comparison between tidal rivers and their resulting fractal dimension. The middle channel was divided up into three sections: the lower, which is just north of the mouth of the Kennetcook River, the middle section, which runs from the mouth of the Kennetcook River south to the start of the upper section which encompasses the mudflats around the Windsor causeway. The three sections within the main channel have unique geomorphic features. The upper section is dominated by large mudflats that are predominantly vegetated, and have channel networks. The middle section has a number of large non-vegetated tidal bars, and the lower section is only dominated by one large formation known as shad bar, which is a large tidal bar that runs from the mouth of the Kennetcook River out towards the centre of the estuary. Each of these sections can be viewed below in figure 6.1.

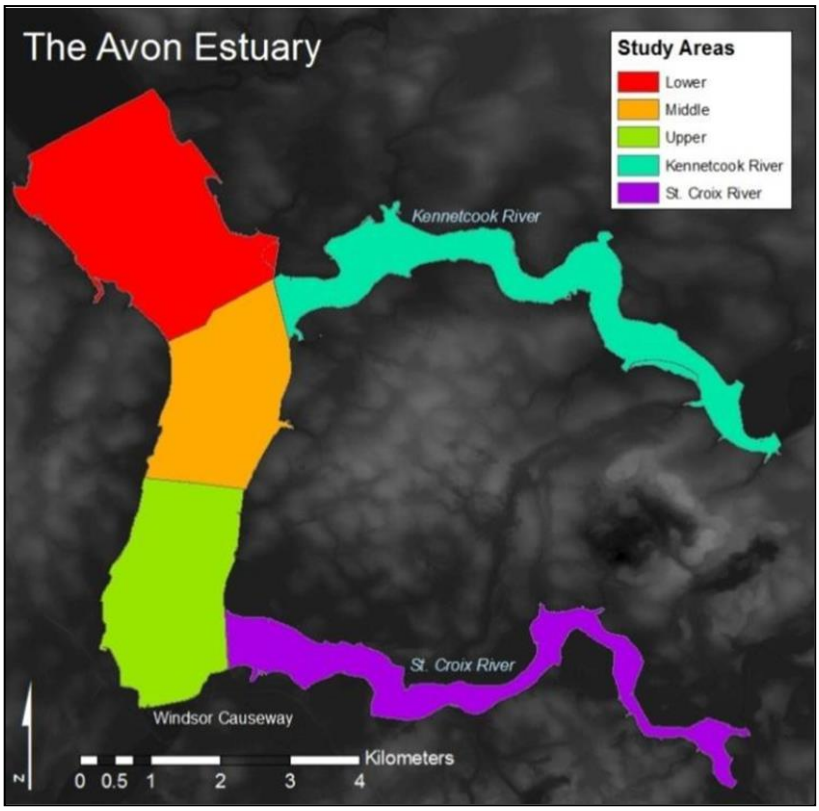

Figure 6.1 Study area of the five sections of the Avon Estuary that were analyzed using the SIM.

6.2 Results of SIM Applied to Sections of the Avon Estuary

6.2.1 Lower Avon

The Lower Avon is the furthest downstream location of the five study areas and has the flow converging from the upper section of the Avon Estuary and the Kennetcook River. The converging flows result in the lower section being dominated by a large channel flow which is visible to the left portion of the river in figure 6.2 and by a large tidal bar extending from the mouth of the Kennetcook River. This section also had the fewest elevation ranges that could be analyzed using the SIM as only 9 of the 26 elevations had at least 5 islands distributed over one order of magnitude which was the minimum cut-off requirement chosen for this study (Chapter 5). The islands analyzed were

between elevations of -5 and -2 m and 6 and 7 m CGVD28 vertical datum.

The lower elevations produced numerous islands along the eastern extent of shad bar. In addition to the islands within the shad bar formation, there was also another series of islands more to the southern portion of the study area. The tidal bars within the lower section are dominated by sand waves with mega ripples which were observed from the LiDAR DEM and from a 2007 Ikonos image.

The higher elevations produced islands along the banks of the estuary and numerous small rivers and streams that feed into the Avon Estuary. The islands are predominantly in areas of high marsh that border the dykes that surround the estuary as shown in figure 6.2.

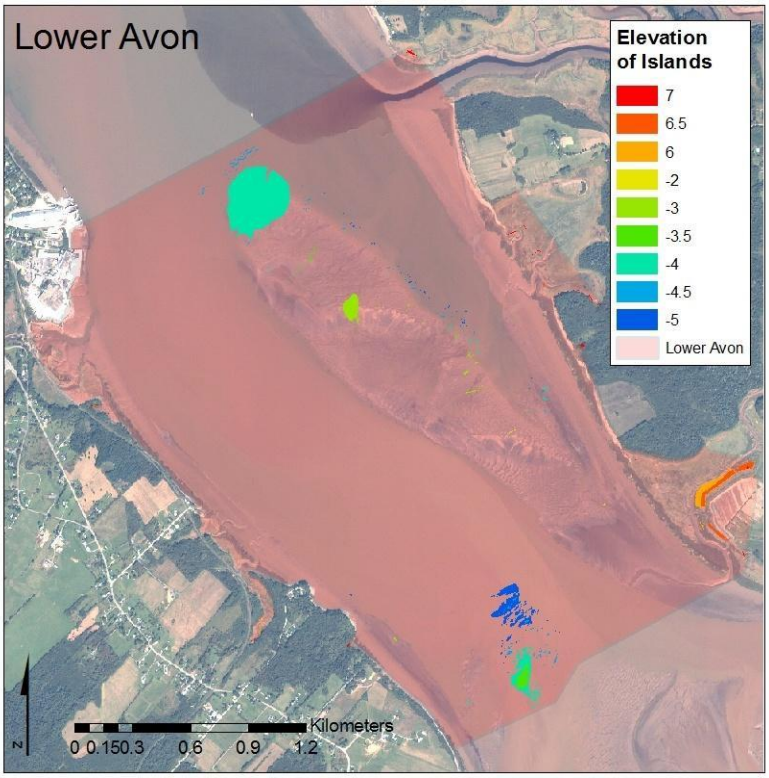

Figure 6.2 Islands used in SIM analysis of the Lower Avon overlaid on an Ikonos Image from 2007.

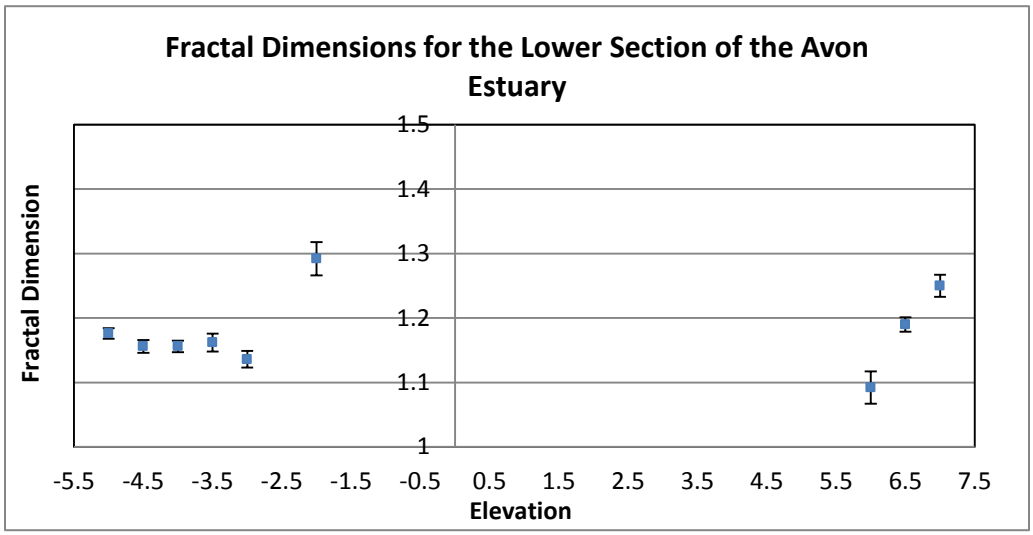

Figure 6.3 Fractal dimension from SIM applied to the lower Avon. The error bars show the standard error of the slope.

The results of the SIM applied to the lower Avon are shown in figure 6.3. The fractal dimensions remain similar between -5 and -3 m with the fractal dimension fluctuating between 1.14 and 1.18 and the islands range over 3 to 4 orders of magnitude. The islands between -5 and -3 m come from two dominant tidal bars that are present within a study area: the shad bar and a smaller bar to the south. Both of these tidal bars are dominated by mega ripples (Pelletier and McMullen, 1972). This environment has continuous redistribution of sediment and the morphology can change with each passing tide. There is a clear spike in the fractal dimension at -2 m, as it rises to 1.29. It is important to note that the islands in the lower section at -2 m ranged just over one order of magnitude, which was the lowest range in magnitude for all of the recorded elevations within the lower section. However, unlike the islands from lower elevations, all of the islands that were captured at this elevation came from two large sand waves that form on the shad bar near the mouth of the Kennetcook River.

The elevations between -1.5 and 5.5 m failed to yield at least 5 islands which was the minimum number of islands needed for analysis. The islands from higher elevations of 6 to 7 m were from areas dominated by marshes which surrounded tidal streams that feed into the estuary. There was another clear spike in the fractal dimension of islands within the upper limits as the fractal dimension jumped from 1.09 at 6 m to 1.19 at 6.5 m and then up to 1.25 at 7 m. Islands that form within this range are often within areas of high marsh and at the upper elevation limit of the study near 7 m. The high marsh within these areas is restricted by dykes that were used to reclaim farm land and have altered the natural flow of water.

6.2.2 Middle Avon

The middle section of the Avon Estuary is between the upper and lower sections. The middle offered four more elevations than the lower section as 13 of the 26 elevations had at least 5 islands spanning over one order of magnitude. The elevations that did not produce enough islands were between -5 m and 4 m. Like the lower section the lower elevations produced islands along large tidal bars that are continuously subject to redistribution of sediment. At 4 m the islands form a more depositional environment on mudflats that extend out from the river banks. The mudflats along the banks also have distinct channels. At 6.5 and 7 m the islands form along the river bank in areas of high marsh which are restricted by dykes (Figure 6.4).

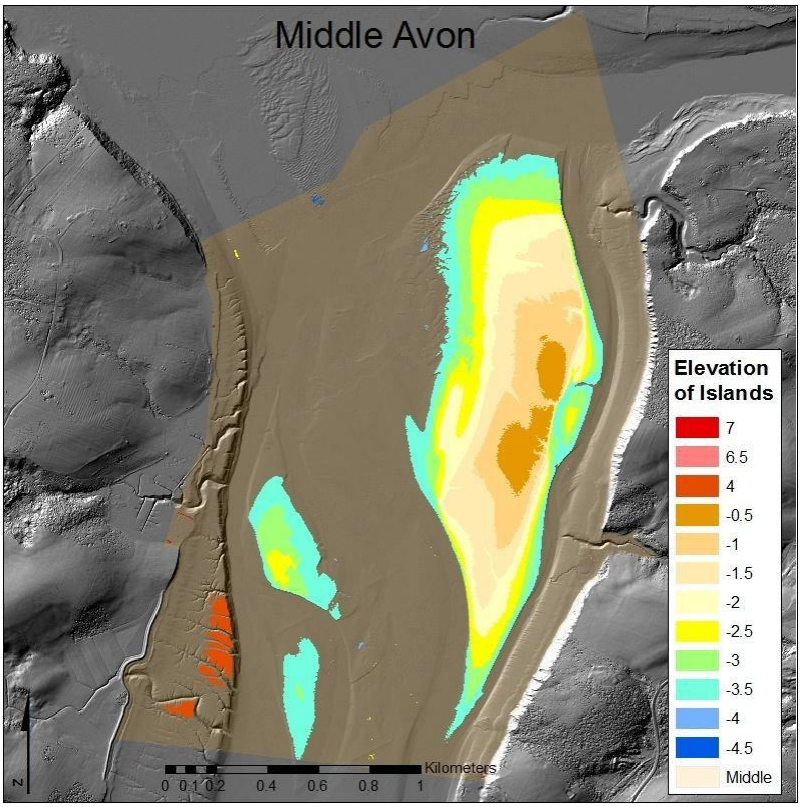

Figure 6.4 Islands used in SIM analysis of the Middle Avon overlaid on an Ikonos Image from2007.

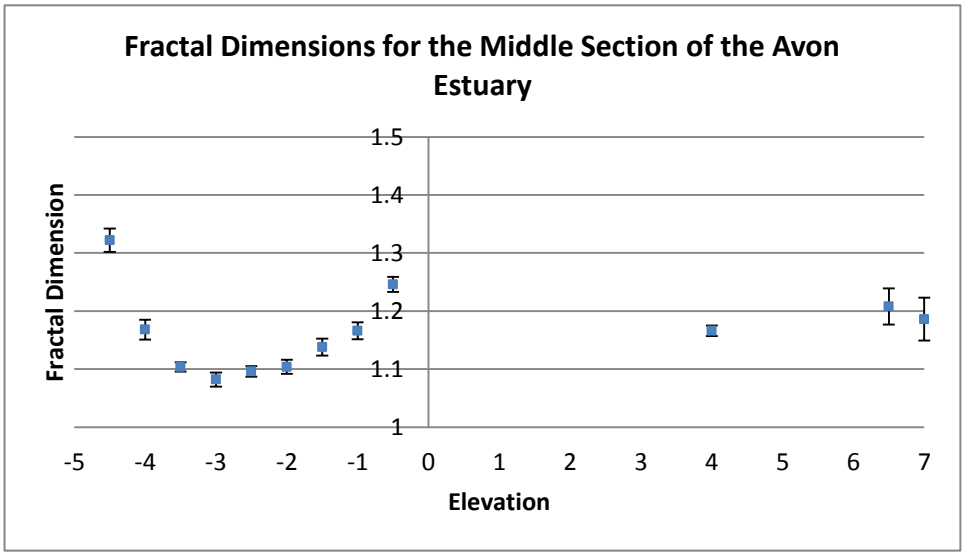

Figure 6.5 Fractal dimension from SIM applied to the middle Avon with error bars showing the standard error of the slope.

The results of the SIM applied to the middle section of the Avon are shown in figure 6.5. The fractal dimension for an elevation of -4.5 m was 1.32 and the scaling ranged over 2 orders of magnitude. The islands that were captured in this range came from large sand waves found on a tidal bar in the middle of the channel. Fractal dimensions between -3.5 and -2 m, fluctuated between 1.08 and 1.10, and the islands range over 4 to 5 orders of magnitude. The islands between -3.5 and -2 m come from three dominant tidal bars that are present in the study area. Similar to the tidal bars at the lower section they are under a continuous redistribution of sediment with each passing tide. The fractal dimension above an elevation of -2 m to -0.5 m increased and the islands were found on the largest tidal bar, within this section. The elevations between 0 to 3.5 m failed to yield at least 5 islands for analysis, often only producing one or two islands. At 4 m the islands came from mudflats on the western side of the estuary and at higher elevations from 6 to 7 m the islands form in areas of high marshes. The high marsh areas surround tidal streams that feed into the estuary and along the banks of the estuary itself.

6.2.3 Upper Avon

The upper section of the Avon Estuary encompasses the Windsor causeway and the mouth of the St. Croix River. The upper section had 16 elevations within the tidal range with islands over at least one order of magnitude which was the cut off for the analysis. The islands that were analyzed were between elevations of -3 and -0.5 m and 2.5 to 7 m. Like the middle and the lower section, the lower elevations produced islands along large tidal bars that are under a constant state of redistribution of sediment. From -3 m to -1 m the majority of the islands form on tidal bars dominated by sand waves and unidirectional

ripples. Above -0.5 m the islands form on mudflats both vegetated and non-vegetated and are in a more depositional environment. At 4 m the islands form on mudflats in areas dominated by vegetation, while above 6 m the islands form along the dykes and mudflats in areas of high marsh as shown in figure 6.6.

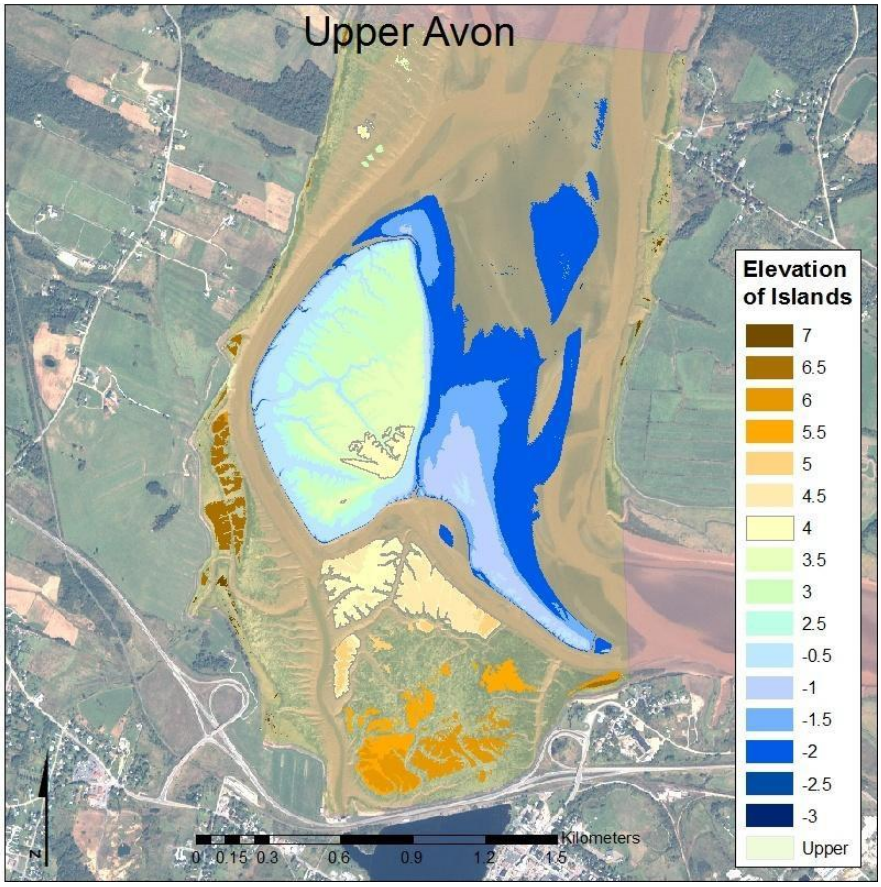

Figure 6.6 Islands used in SIM analysis of the Upper Avon overlaid on an Ikonos Image from 2007.

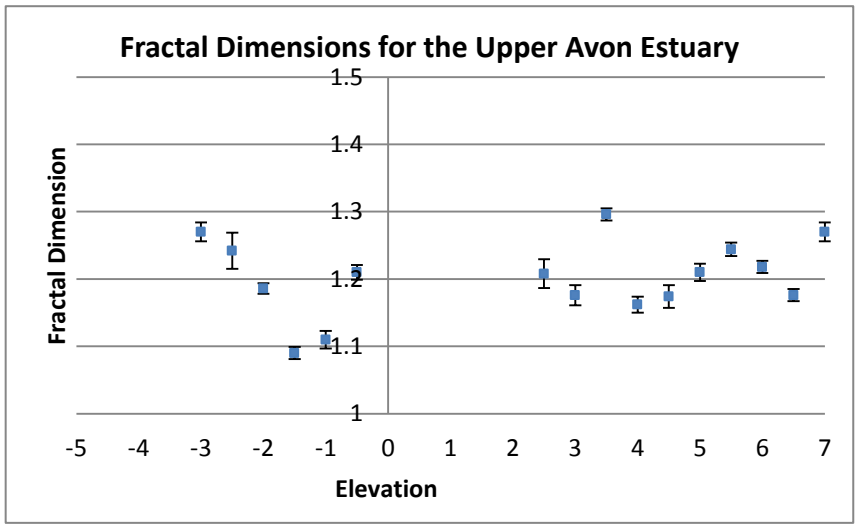

Figure 6.7 Fractal dimension from SIM applied to the upper Avon with error bars showing the standard error of the slope.

The results of the SIM applied to the upper section of the Avon are shown in figure 6.7. The fractal dimension for elevations from -3 m to -1 m had a relatively constant decrease in value with an increase in elevation. The islands that were captured in this range came from large tidal bars in the middle of the channel, and the largest tidal bar had a tidal creek thalweg that stretched towards the mouth of the St. Croix River. This section is quite different from what was found for the lower and middle section where the fractal dimension remained relatively the same at this elevation range. The fractal dimensions rose to just above 1.2 at -0.5 m and the remaining elevation from 2.5 m to 7 m fluctuated around 1.2. At 4 m the fractal dimension was 1.6 and the islands formed on mudflats. The fractal dimension increased with elevation until an elevation of 5.5 m, which is near the HHWL of 5.7 m (van Proosdij, 2007) with a D value of 1.24. The fractal dimension decreased with elevation above 5.5 m to 6.5 m up to a level of 7 m. At 7 m the fractal dimension had a clear increase from 1.18 to

1.27. The islands at 7 m are restricted by dykes, which are along the banks of the estuary and the causeway.

6.2.4 Kennetcook River

The Kennetcook River drains into the lower section of the Avon Estuary. This section had 17 elevations within the tidal range with islands over at least one order of magnitude, which was the cut off for the analysis. The islands analyzed were between elevations of -4.5 to 2 m and from 6.5 to 7 m. The islands formed on a series of tidal bars within the river, along the river banks and also in areas of high marsh, which were further up the banks in front of dykes. The largest tidal bar formed near the mouth of the Kennetcook River and had an elevation range from -4.5 m to 7 m. This was the largest elevation range of any tidal bar within the Avon Estuary. At the lower elevations, between -4.5 m and -3 m, the islands formed on large sand waves (Figure 6.8) within the lower section of the Kennetcook River. For the most part the islands between -2.5 m and 2 m form on tidal bars within the river. At 6.5 m the islands form in areas of high marsh along the banks. At 7 m the islands are being restricted by the dykes alongside river banks (Figure 6.8).

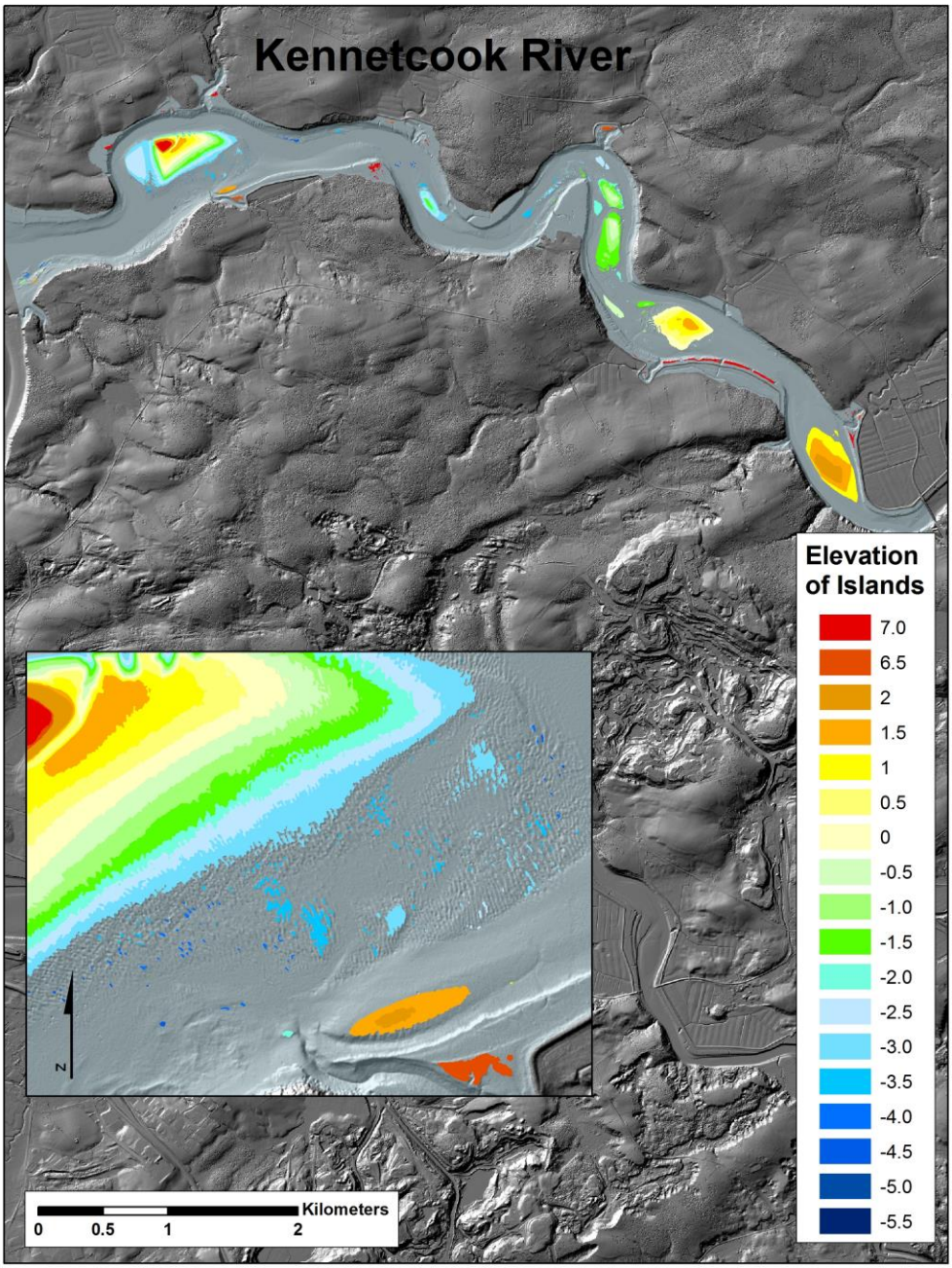

Figure 6.8 Islands used in SIM analysis of the Kennetcook River overlaid on a hill shade of 2007 LiDAR survey and are color coded base on their fractal dimension for each elevation.

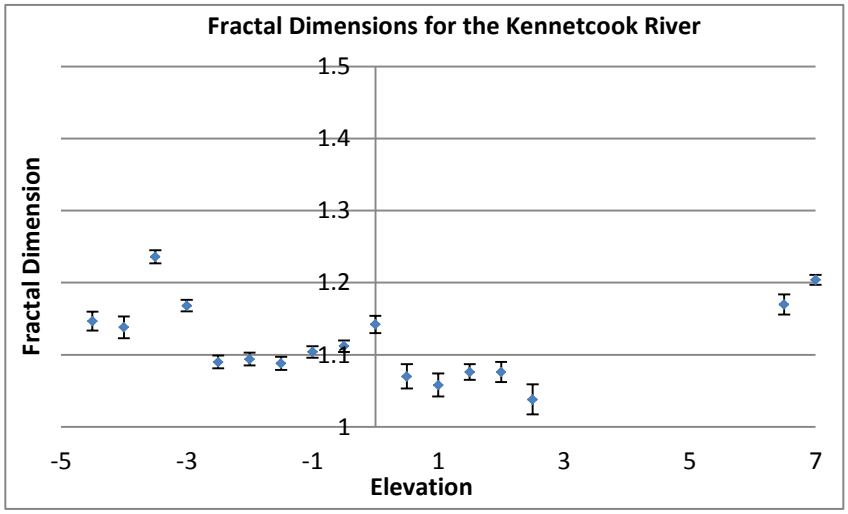

Figure 6.9 Fractal dimension from SIM applied to the Kennetcook River with error bars showing the standard error of the slope.

The results of the SIM applied to the Kennetcook River are shown in figure 6.9. The fractal dimensions for elevations from -4.5 m to -3 m were higher compared to the results from the other elevations other than at an elevation of 6.5 and 7 m. The islands between -4.5 and -3 m mostly formed on sand waves (Figure 6.8) with a fractal dimension range between 1.14 and 1.24. The remaining islands between -2.5 m and 2.5 m form on tidal bars throughout the Kennetcook River, and their fractal dimensions range between 1.04 and 1.14 with most of the elevations having a fractal dimensions closer to 1.1. Between 3 m and 6 m there were fewer than 5 islands, which was the minimum amount of islands chosen to be used for the analysis, or the range in scale was less than 1 order magnitude. There is a noticeable increase in the fractal dimension from 6.5 to 7 m, i.e from a fractal dimension of 1.1 to 1.2. At 7 m the islands were being limited by dykes along the river banks.

6.2.5 St. Croix River

The St. Croix River drains into the upper section of the Avon Estuary near the Windsor causeway. The area used in the analysis extended from the mouth of the St. Croix River to the Avondale road bridge. There were only 13 elevations within the tidal range that had results over at least one order of magnitude. The islands that were analyzed were between elevations of -2.0 to 3.5 m and from 6.5 to 7 m. Similar to the Kennetcook River the islands formed on a series of tidal bars within the river, along the river banks and also in areas of high marsh along dykes. Unlike the Kennetcook River, the larger tidal bar formed further downstream within the river. The lower elevations, between -2.0 m and -0.5 m, formed on tidal bars that were present over multiple elevations. For the most part the islands between -2.5 m to -2 m form on tidal bars near the mouth of the river and do not have islands at higher elevations above them. Islands between 0.5 m and 3.5 m form on tidal bars through the St. Croix River and also along the river banks (Figure 6.10). At 6.5 m the islands start to form in areas of high marsh along the river banks. At 7 m the dykes which run along the estuary restrict the island lateral growth as they act as a barrier (Figure 6.10).

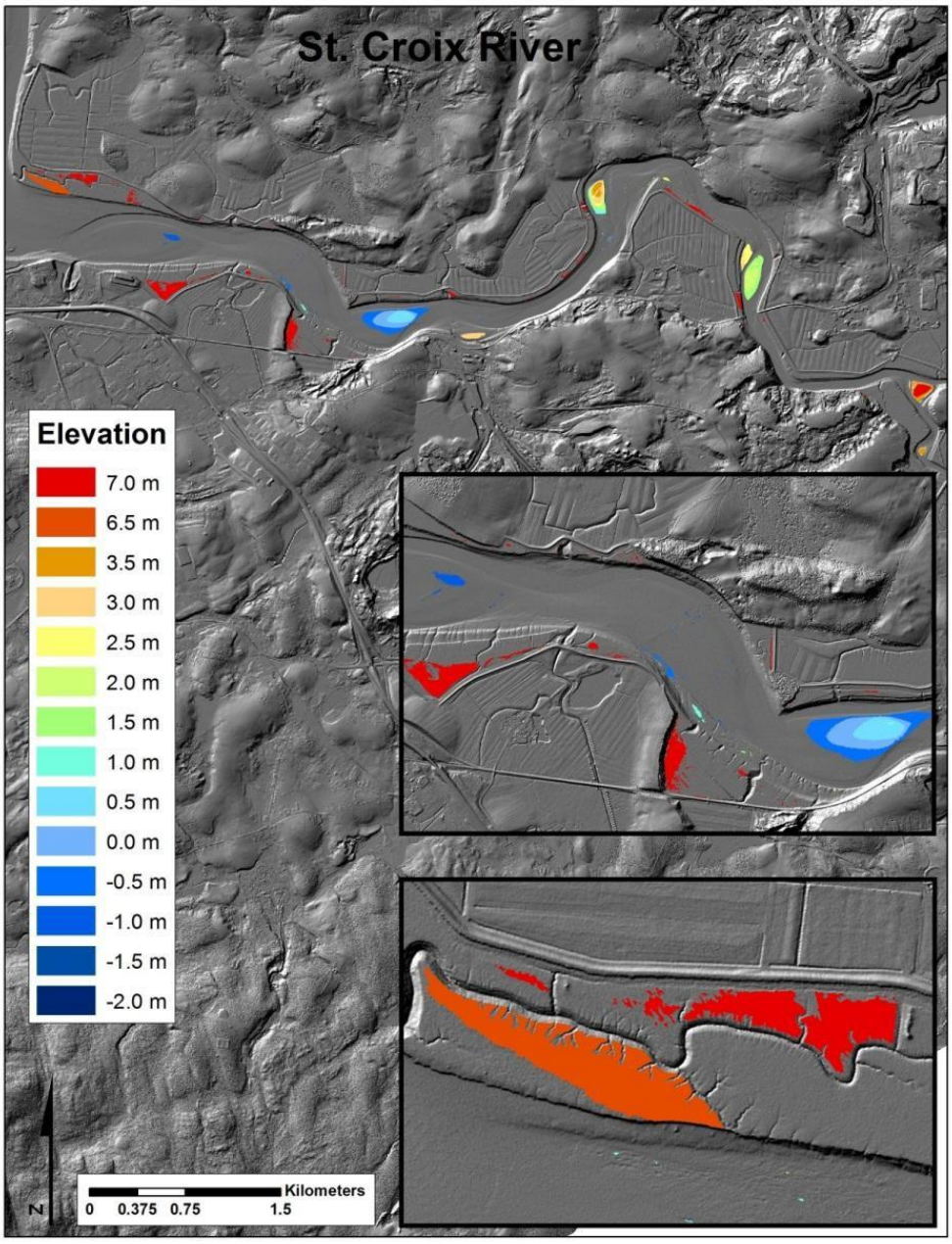

Figure 6.10 Islands used in SIM analysis of the St. Croix River overlaid on a hill shade of 2007 LiDAR survey. The two inset maps increase variability of the shape of the islands at 6.5 m and 7 m compared to the islands found at the lower elevations 2 m to – 0.5 m.

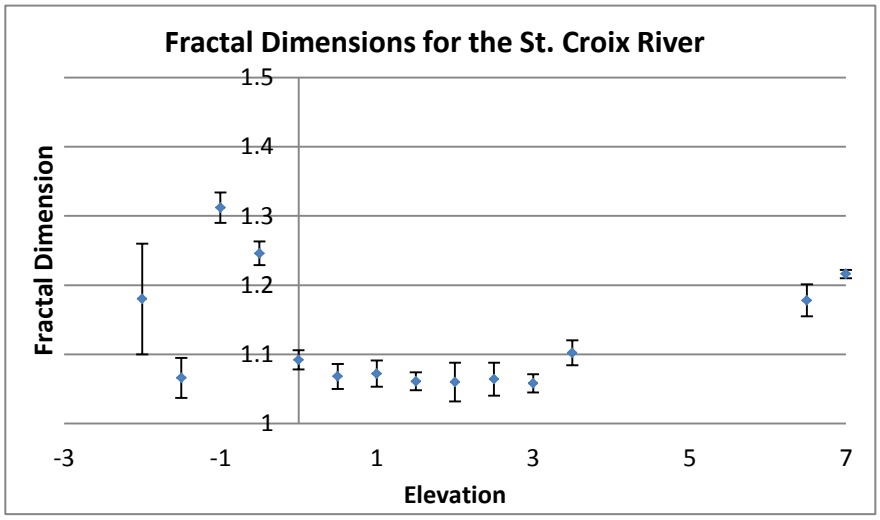

Figure 6.11 Fractal dimension from SIM applied to the St. Croix River with error bars showing the standard error of the slope.

The results of the SIM applied to the St. Croix River are shown in figure 6.11. Similar to the islands within the Kennetcook River the islands that form at the lower elevations within the St. Croix had higher fractal dimension then those in the middle elevation range. Islands between 0.0 m and 3.5 m form on tidal bars and the banks throughout the St. Croix River. The resulting fractal dimensions for the middle elevations range between 1.06 and 1.10 with most of the elevations having a fractal dimension closer to 1.06. From 0.5 m to 3.0 m there is almost no change in the fractal dimension. There is, however, a noticeable increase in the fractal dimensions at 6.5 m and 7 m. At this elevation range the islands form within areas of high marsh along the river banks. The resulting fractal dimension for these areas of high marsh was 1.18 and 1.22. Like the other sections analyzed at 7 m the islands were being impacted by the dykes along the river banks.

6.3 Discussion

Three subsections of the main channel of the Avon Estuary were analyzed separately along with the Kennetcook and St. Croix Rivers. Applying the SIM to subsections of the Avon Estuary presented challenges in comparing the results, as there were not always 5 islands distributed over at least one order of magnitude which was the chosen minimum requirement. Since the SIM is restrained to only consider those contours that are closed, the islands that are produced represent only the natural formations of tidal bars and mud flats within the studied portion of the estuary.

The use of other fractal analysis methods that analyzed all contours, not just closed ones, such as the divider method (Andrle, 1996) or Box Counting (Legendre et al., 1994) may prove more beneficial than the Slit Island method when analyzing smaller areas within the Avon Estuary. Out of the 26 elevations there were only three elevations that produced enough islands in each of the subsections which could be used for comparison. The three elevations that were comparable within the main channel were; -2 m, 6.5 m, and 7 m. The table below shows the fractal dimension for all five subsections of the Avon Estuary along with the results from the entire Avon Estuary presented in chapter four (Figure 6.12).

	Elevation		
Section	-2 m	6.5 m	7.0 m
St. Croix River	1.18	1.18	1.22
Kennetcook River	1.09	1.17	1.20
Lower Main Channel	1.29	1.19	1.25
Middle Main Channel	1.10	1.21	1.19
Upper Main Channel	1.19	1.18	1.27
Entire Avon	1.29	1.21	1.28

Table 6.1. The above table provides fractal dimensions for the five subsections of the Avon Estuary, and the entire Avon Estuary presented in chapter four, for -2 m, 6.5 m and 7 m.

Table 6.1 shows that the fractal dimension varies within the Avon Estuary for all three elevations, however, the largest difference is found at -2 m as there is a difference of 0.2 in the fractal dimension between the Lower Main Channel and the remaining subsections. The largest amount of islands with an elevation of -2 m is found within the Lower Main which also spans over 5 orders of magnitude.

For the 6.5 m elevation, the difference in fractal dimension was less pronounced as subsections were within 0.04 of each other. Inspection of the islands, using Ikonos imagery from 2007 of the Avon Estuary, showed that at 6.5 m islands are forming within vegetated areas along the banks of the estuary for all five sections.

At 7 m elevation the fractal dimensions were within 0.09 of each other with the highest value coming from the Upper Main Channel around the Windsor causeway. The islands at the 7 m range were also forming in areas of vegetated marsh along the banks of the estuary. Due to the low number of comparable elevations, the results for the three subsections within the Main Channel were compared against the results of the entire Main Channel presented in chapter four (Figure 6.12).

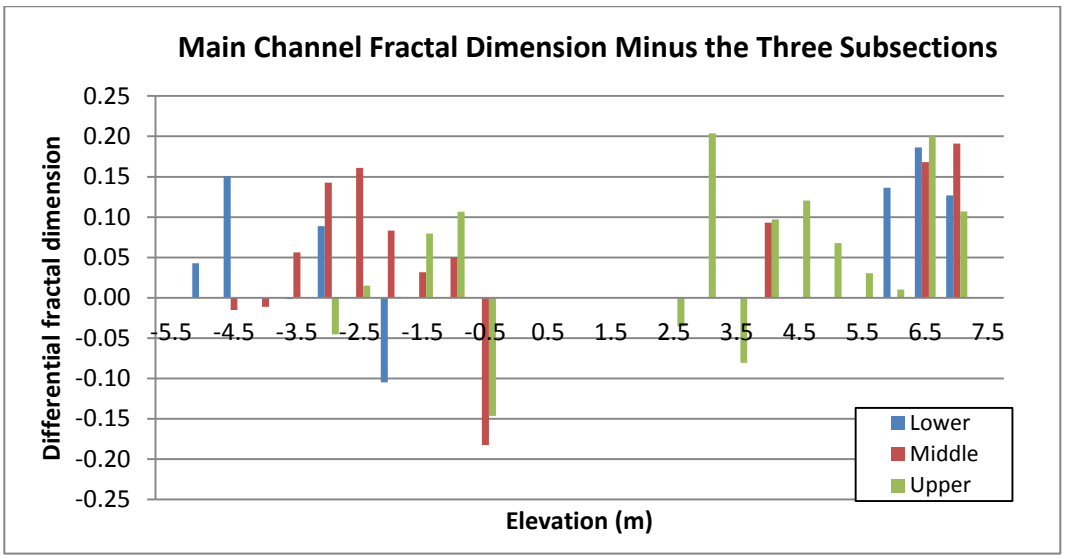

Figure 6.12 The Y axis is the difference between the fractal dimensions of subsections of the Main Channel to the entire Main Channel for elevations shown on the X axis.

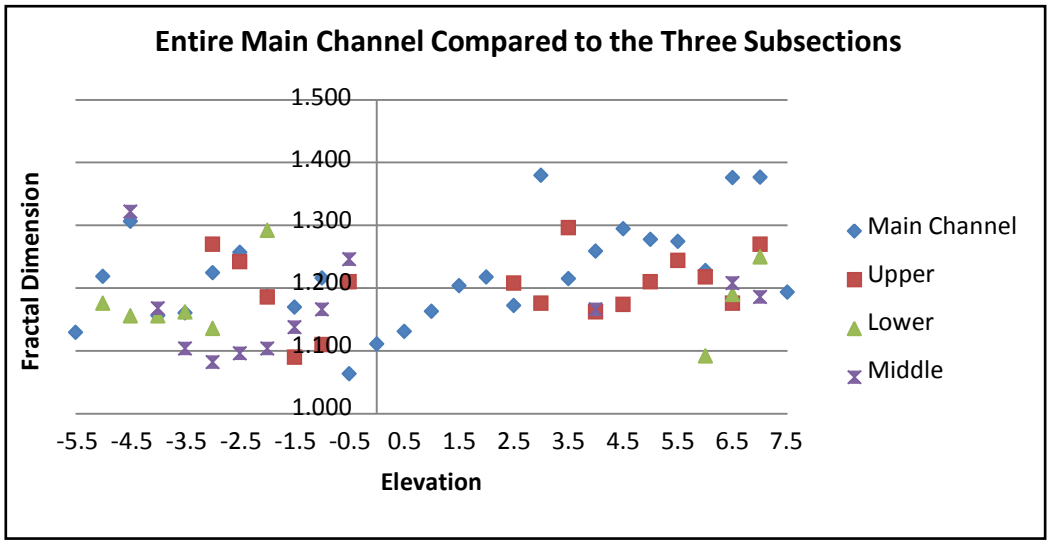

Figure 6.13 Fractal dimension of subsections of the Main Channel compared to entire Main Channel.

Comparing the fractal dimension of the subsections of the Main Channel shows the spatial variability in the fractal dimension within the main channel. The differences between the fractal dimension of the subsections of the Main Channel were as high as 0.2 compared to the entire section (Figure 6.12). The difference in the fractal dimension for a given elevation between the subsections of the main channel suggests that at that elevation the different subsections may have other processes dominating the formation of islands.

The St. Croix and the Kennetcook Rivers had 12 elevations with enough islands spanning over at least one order of magnitude that could be compared as (Table 6.2)

Elevation (m)	St. Croix River	Kennetcook River	Difference
-2	1.18	1.09	0.09
-1.5	1.07	1.09	-0.02
-1	1.31	1.10	0.21
-0.5	1.25	1.11	0.13
0	1.09	1.14	-0.05
0.5	1.07	1.07	0.00
1	1.07	1.06	0.01
1.5	1.06	1.08	-0.02
2	1.06	1.08	-0.02
2.5	1.06	1.04	0.03
6.5	1.18	1.17	0.01
7	1.22	1.20	0.01

Table 6.2 Comparing the fractal dimensions for the St. Croix River and the Kennetcook River at varying elevations within the tidal range.

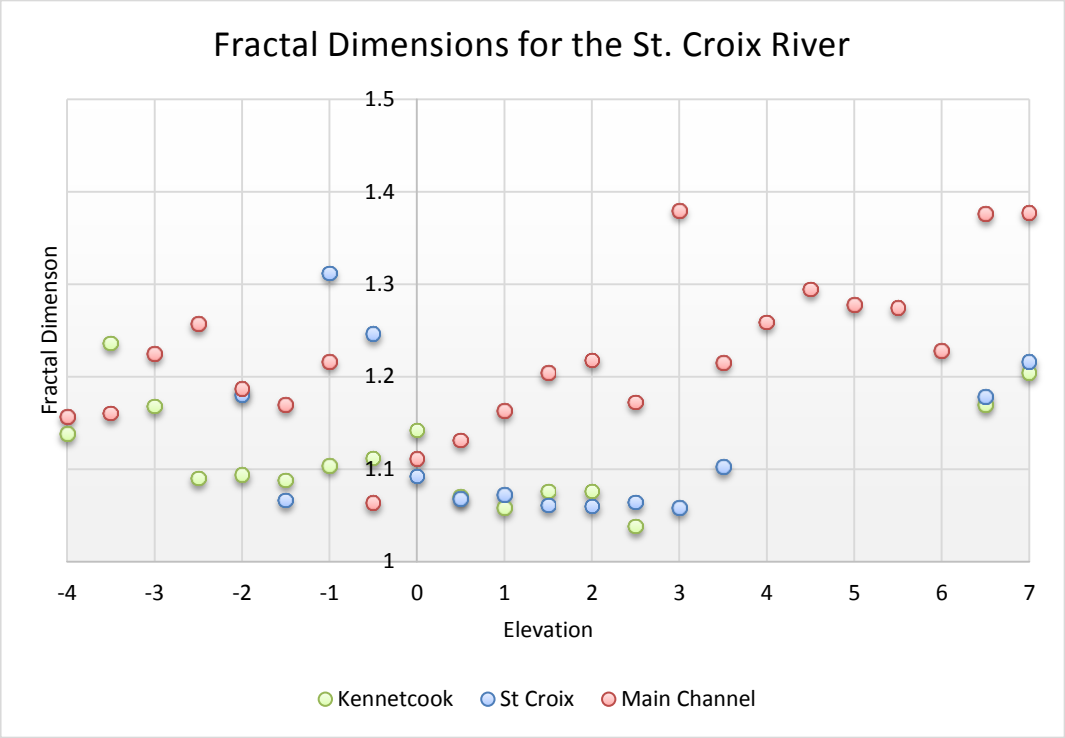

Figure 6.14. Fractal dimension of St. Croix River, Kennetcook River and Main Channel.

The fractal dimension of both Kennetcook and the St. Croix River were similar above 0 m with the largest difference being 0.03 (Table 6.2). Over this range from 0 to 2.5 m the islands within the river systems are forming as sand bars, whereas in the main channel the islands are part of well-established mud flats with vegetation and channel networks. This difference may explain why the fractal dimension was higher for the main channel as the vegetation and channel networks in the upper section are more resistant to the directional flow of the water and thus results in more irregular formations of islands. Below 0 m the difference in fractal dimension was as high as 0.21 occurring at an elevation of -1 m. The islands that form at -1 m within the St. Croix had no other islands forming vertically above them, unlike the islands for the same elevation within the Kennetcook River. This may suggest that the islands within

the St. Croix at -1 m are more susceptible to change with each passing tide than those forming within the Kennetcook River that appear to be more permanent formations.

6.4 Conclusion

The study showed that there were two distinct systems, the main channel and tidal rivers as the fractal dimension from the both of the river systems differed from the results of the main channel (Fig. 6.14). The fractal dimensions at higher elevation (above 0 m) were very similar, with the largest difference being 0.05 at 0 m. This is likely due to the islands at these ranges being further up the river system and as a result having less interaction with the main channel.

Chapter 7 Conclusions

This study investigated the Avon Estuary assessing the relationship that tidal elevation and processes play in the geomorphology of the Avon Estuary. The study relied on the use of the SIM, which is a type of multi-scale analysis, and was applied to a high resolution DEM. The DEM was produced from Airborne Laser Scanning (ALS), which allowed for a wider range in spatial scale to be considered than other available data sources that are at coarser resolutions. The 3D self-similarity of intertidal zones was assessed along with possible links between physical processes that may affect morphology at certain elevations (chapter 4). The interpolation method was considered as it had the potential to influence the results of SIM (chapter 5) and lastly the impacts on the fractal dimension when constraining the study area were investigated (Chapter 6). Chapter 4 demonstrated that the inter-tidal zone within the Avon Estuary was not a 3D isotropic self-similar system as the fractal dimension was not the same over all elevations within the tidal range. This is an important finding as fractal analysis has often been applied in previous studies (Dai, 2004; Mandelbrot, 1967) only considering delineated coastlines from air photos, satellite imagery and charts, which were two-dimensional, and did not account for variation in elevation. The dependence on elevation probably arises due to different geomorphic processes dominating the formation of landforms at various elevation ranges.

The fractal dimension for SIM is determined based on the power law relationship between the areas of the islands and their perimeters. There was strong correlation for the power laws from each of the elevations that SIM was applied to, with correlation

coefficients frequently being higher than 95%. Added to the wide range of scales on which the power was found valid, the strong correlation provided a high degree of confidence that the results did reflect broad characteristics of the pattern and not just local morphological details. The fractal dimension ranged from 1.0 to 1.38, which represents a wider range than those previously observed in similar tidal environments (Schwimmer, 2008). The height dependence of the fractal dimension did not appear to be random (chapter four). The fractal dimensions within the Avon Estuary typically decreased with an increase in elevation from -5 m to 0.5 m followed by a plateau to 2.5 m before rising again. The fractal dimensions, for the Avon estuary, fluctuated around 1.2 from -5m to -2m, at this elevation range the system is dominated by a high flow velocity as the tidal waters are restricted by intertidal bodies (Lambiase, 1980) and the distribution of sediment results in the formation of intertidal sand bars dominated by sand waves and mega ripples (van Proosdij 2007). The form of these tidal sand bars changes with each passing tide. Between -2 and -1 m bidirectional ripples appear within the tidal bars, as fine sediment is deposited. The resulting fractal dimension is around 1.8. Due to tidal flow above -0.5 m to around 1.5 m the tidal bars become more elongated and medium to coarse sediment starts to deposit. The elongated tidal bars result in the formation of smoother islands causing a lowering of the fractal dimension which fluctuates around 1.13. The system changes to a more depositional environment above 1.5 m and there is a clear establishment of channel networks within the mud flats resulting in a change in pattern of fractal dimension to now increase with elevation. Beyond 2.5 m the rate in which the fractal dimension increases with elevation lessens as vegetation becomes dominant within the mud flats, resulting in a more stabilized

environment, preserving the shape of the channel networks. The Avon Estuary showed that depositional environments where vegetation is established can have more complex shape than that of erosional zones.

Chapter 5 assessed the dependence of the SIM on the type of interpolation method that was used in production of the DEM being assessed. The three interpolation methods that were evaluated were Spline, Natural Neighbor and IDW. The fractal dimension for a given elevation within the study area varied with the interpolation method, proving that the interpolation method does have an influence on the results when running the SIM. The finding is similar to what Gilbert (1998) found when applying a power spectra to subsea profiles, in that the interpolated surface did influence the results. However the results from the three DEM using different interpolation methods produce fractal dimensions that followed the same trends in terms of their elevation dependence (Figure 5.9).

The maximum range in the fractal dimension values obtained with the three interpolation methods was 0.23; it was reached at an elevation of negative 2.5 m and the second highest range was at -4 m and at both of these elevations the correlation coefficients were below 0.90 . The lowest difference between the fractal dimensions for the three interpolation methods was at -1.5 m and 5.5 m. The resulting correlation coefficients at -1.5 m and 5.5 m were above 0.95. There were unique qualities to each of the interpolation methods. The fractal dimensions generated from the Spline DEM were frequently the highest compared to those from IDW and Natural Neighbor DEMs (Figure 5.10). Natural Neighbor produced the lowest fractal dimension for 13 of the 22 elevations assessed. IDW DEM had the least amount of elevation ranges that did

produce enough islands to be used in the analysis.

The differences in the fractal dimension from each interpolation method highlights the importance of stating the interpolation used when preforming fractal analysis. It can also explain differences in the fractal dimension when comparing multiple surveys of the same area. If the interpolation method used is not the same for each study and or the data source has different point spacing then this will have a direct effect on the interpolation surface and could have an effect on the resulting fractal dimension. Chapter 6 showed that there are limitations to the SIM when applying it to smaller subsection within the Avon Estuary. The Avon Estuary was broken into 5 subsections; three within the main channel and one for each of the tidal rivers that feed into the Avon Estuary. The main limitation of the SIM was elevation gaps in the analysis, as there were a lack of islands at certain elevation ranges that met the imposed minimum requirements. There were only three elevations out of the 26 elevation ranges that had enough islands for analysis in all 5 subsections (Table 6.1).

The differences for the fractal dimension at -2 m ranged from 1.09 within the Kennetcook River to 1.29 for the Lower Main Channel. However the differences at the higher elevation of 6.5 m and 7.0 m were considerably lower as the range in the fractal dimension was only 0.04 at 6.5 m and 0.09 at 7 m. The higher range in the fractal dimension at the lower elevations is probably due to different processes dominating in the subsections whereas at the higher elevations the main process is constant as it is high marsh through all of the subsections. Given the lack of elevation that had met the imposed minimum requirements for islands to run SIM at more localized levels, other fractal analysis methods may prove to be more useful.

7.1 Recommendations

a. Having multiple data sets from each start of season would allow for seasonal variations within the Avon Estuary to be compared.
b. Applying the SIM to another macro tidal environment which is not being influenced by anthropogenic features such as dykes or a causeway would allow for a comparison between the formations of the resulting mud flats.
c. It is recommended that an error analysis be performed on LiDAR derived DEMs of the Avon Estuary generated with commonly used interpolation methods such as natural neighbor, IDW, Spline and Krigging to determine the optimal interpolation method for a macro tidal environment.
d. Further studies using other fractal dimension methods such as box counting or divider methods would allow for a more refined study area within the Avon Estuary. These methods would also be able to consider contours that did not close within the bounds of the study area and the coast line could be assessed.
e. Finally, a multifractal approach is expected to provide new insights into the studied pattern variability and its relation to geomorphic processes.

Literature Cited

Allen, J.R.L. 2000. Morphodynamics of Holocene saltmarshes: a review sketch from the Atlantic and Southern North Sea coasts of Europe. Quaternary Science Reviews 19: 1155-1231.

Almqvist, N. 1996, Fractal analysis of scanning probe microscopy images, Surface Science, 355, 1-3, 221-228.

Andrle, R., 1994, The angle measure technique: a new method for characterizing the complexity of geomorphic lines, Math. Geology, v. 26, no. 1. p. 83-97.

Andrle, R., 1996. Complexity and Scale in Geomorphology: Statistical Self-Similarity vs. Characteristic Scales, Mathematical Geology, Vol. 28, No. 3.

Athearn, N. Takekawa, J. Jaffe, B. Hattenbach, B., 2010. Mapping Elevations of Tidal Wetlands Restoration Sites in San Francisco Bay: Comparing Accuracy of Arial LiDAR with a singlebeam Echosounder, Journal of Coastal Research Vol. 26 No. 2.

Apaydin, H., Kemal S., Yildirim, E., 2004, Spatial interpolation techniques for climate data in the GAP region in Turkey, Climate Research, Vol. 28: 31–40.

Amos, C. L 1984. The sedimentation effect of tidal power development in the Minas Basin. Bay of Frandy. in D. C. Gordon and M. J. DadsweII (ed.) Update on the marine envircmnental consequences of tidal power development in the upper reaches of the Bay of Fundy. Can. Tech. Rep. Fish. Aquat. Sci. 8 256: 385402.

Baas, C.W., 2002. Chaos, Fractals and Self-organization in Coastal Geomorphology: Simulating Dune Landscapes in Vegetated Environments, Geomorphology 48, 309–328.

Bater, C. W., & Coops, N. C. (2009). Evaluating error associated with lidar-derived DEM interpolation. Computers & Geosciences, 35(2), 289-300.

Burrough, P.A., 1981. Fractal Dimensions of Landscapes and Other Environmental Data, Nature 294, 240–242.

Carr, J.R., 1997. Statistical Self-affinity, Fractal Dimension, and Geologic Interpretation. Engineering Geology 48, 269–282.

Chasmer, L., Hopkinson, C., & Treitz, P. (2006). Investigating laser pulse penetration through a conifer canopy by integrating airborne and terrestrial lidar. Canadian Journal of Remote Sensing, 32(2), 116-125.

Clarke, K. C. (1986). Computation of the fractal dimension of topographic surfaces using the triangular prism surface area method. Computers & Geosciences, 12(5), 713-722.

Daborn, G. R., Brylinsky, M., & van Proosdij, D. (2003). Ecological Studies of the Windsor Causeway and Pesaquid Lake, 2002. Contract, 2, 00026.

Dalrymple, R.W.; Knight, R.J.; Zaitlin, B.A.; and Middleton, G.V. 1990. Dynamics and facies model of a macrotidal sand-bar complex, Cobequid Bay – Salmon River Estuary (Bay of Fundy). Sedimentology 37: 577-612.

Dai, Z.J., Li, C.C, Zhang, Q.L., 2004. Fractal Analysis of Shoreline Patterns for Crenulate- bay Beaches, Southern China, Estuarine, Coastal and Shelf Science 61 65-71.

Dend, Y., 2007. New Trends in Digital Terrain Analysis: Landform Definition, Representation, and Classification, Progress in Physical Geography, 31, 405-419.

Desplanque, C. and Mossman 2004. Tides and their seminal impact on the geology, geography, history, and socioeconomics of the Bay of Fundy, eastern Canada. Atlantic Geology 40 (1): 1-130.

Droppo, I.G., Ongley, E.D. 1992, The state of suspended sediment in the freshwater fluvial environment: a method of analysis, Water Research, 26, 1:65-72.

ESRI, 2010. ArcGIS 9.3, Help Documentation. New York, ESRI.

Family, F., Vicsek, T., 1991. Dynamics of Fractal Surfaces, World Scientific, Singapore, 1, 3.

Friedrichs, C.T. Perry J.E., 2001. Tidal Marsh Morphodynamics: A Synthesis. Journal of Coastal Research 27:7-37.

Gao, Y., 2009, Algorithms And Software Tools For Extracting Coastal Morphological Information From Airborne LiDAR Data, MSc Thesis Office of Graduate Studies, Texas A&M University.

Garroway, K. (2010). An Airborne Laser Scanning Approach to Mapping and Modelling Surface Moisture in an Agricultural Watershed in Nova Scotia.

Gilbert, L.E., 1989, Are topographic data sets fractal, Pure and Applied Geophysics, Volume 131.

Glenn, N.F., Streutker, D.R., Chadwick, D.J., Thackray, G.D., Dorsch, S.J., 2006. Analysis of LiDAR-derived topographic information for characterizing and differentiating landslide morphology and activity, Geomorphology, 73, 1-2.

Goodchild, M.F., 1980, Fractals and the Accuracy of Geographical Measures.

Mathematical Geology Vol.12, pp 85–98.

Goodchild, M.F., Gopal, S. 1989, Accuracy of spatial databases, New York: Taylor and Francis.

Goulden, T. 2009, Prediction of Error Due to Terrain Slope in LiDAR Observations, MSc Thesis Department of Geodesy and Geomatics Engineering, University of New Brunswick.

Han, M., Sun, Y., Xu, S. 2007, Characteristics and driving factors of marsh changes in Zhalong wetland of China, Environmental Monitoring and Assessment, 127, 1-3:363-381, DOI: 10.1007/s10661-006-9286-6.

Hopkinson, C., Demuth, M., Sitar, M., Chasmer, L., 2001, Applications of Airborne LiDAR Mapping in Glacierised Mountainous Terrain, Geoscience and Remote Sensing Symposium, 2001. IGARSS '01. IEEE 2001 International, Vol: 2, 949-951.

Ioana, C., Munteanu, F., Suteanu, C. 1997, Smoothing dimensions analysis—new effective tools in fractal signal investigation, in Fractal Frontiers: Fractals in the Natural and Applied Sciences, eds. M. M. Novak and T. G. Dewey, Singapore: World Scientific, 81–90.

James, T.D., Carbonneau, P.E., Lane, S.N., 2007, Investigating the effects of DEM Error in Scaling Analysis, Photogrammetric Engeneering & Remote Sensing, Vol. 73, No.1, January, pp.67-78.

Jiang, J. Poltnick, R. 1998, Fractal Analysis of the Complextity of United States Coastlines, Mathematical Geology, Vol. 30.

Krummel, J.R., Gardner, R.H., Sugihara, G., O'Neill, R.V., Coleman, P.R. 1987, Landscape patterns in a disturbed environment, Oikos, 48:321-324.

Kennet, M., & Eiken, T., 1997, Airborne Measurement of Glacier Surface Elevation by Scanning Laser Altimeter. Annals Glacial, 24, 235 – 238.

Kojima, N., Laba, M., Ximena, M., Liendo, V., Bradley, A.V., Millington, A.C., Baveye, P., 2006. Causes of the Apparent Scale Independence of Fractal Indices Associated with Forest Fragmentation in Bolivia, ISPRS Journal of Photogrammetry & Remote Sensing, Vol. 61, pp 84–94.

Lambiase, J.J., 1980. Sediment dynamics in the macrotidal Avon River estuary, Bay of Fundy, Nova Scotia. Canadian Journal of Earth Science, 17:1628-1641.

Legendre, F.H.P., C. Bellehumeur, Lafrankie, J.V. Diversity Pattern and Spatial Scale: A Study of a Tropical Rain Forest of Malaysia, Environment Ecology Statistics, Vol. 1 pp. 265–286.

C.P.Lo Albert K.W.Yeung, "Concepts and techniques of Geographic Information Systems", Prentice-Hall of Upper Saddle River, New Jersey, 2002
Mandelbrot, B. 1967, How Long Is the Coast of Britain? Statistical Self-Similarity and Fractional Dimension. Science, New Series, Vol. 156, No. 3775. (May 5, 1967), pp. 636-638.

Mandelbrot, B. Passoja, D. Paullay, A. 1984, Fractals character of fracture surface of metals, Nature,Vol: 308.

Mark, D.M., Aronson, P.B., 1984, Scale-Dependent Fractal Dimensions of Topographic Surfaces: An Empirical Investigation, with Applications in Geomorphology and Computer Mapping, Mathematical Geology, Vol. 16, No. 7.

Nason, G. P. "Stationary and non-stationary times series." Statistics in Volcanology. Special Publications of IAVCEI 1 (2006): 000-000.

Nova Scotia Department of Agriculture and Marketing (NSDAM). 1987. Maritime Dykelands: the 350 Year Struggle. Department of Government Services Publishing Division, 110 pp.

Pan, W.-B., Li, D.-F., Tang, T., Cai, Q.-H. 2003, The fractal character of lake shoreline and its ecological implications, Acta Ecologica Sinica, 2003, 12, DOI: cnki:ISSN:1000-0933.0.2003-12-027.

Pérez-López, R., & Paredes, C. (2006). On measuring the fractal anisotropy of 2-D geometrical sets: Application to the spatial distribution of fractures. Geoderma, 134(3), 402-414.

Poljacek, S.M., Risovic, D., Furic, K., Gojo, M. 2008, Comparison of fractal and profilometric methods for surface topography characterization, Applied Surface Science, 254:3449-3458

Olsen, L., Chaudhuri, P., Godtliebsen, F., 2007. Multi-scale Spectral Analysis for Detecting Short and Long-range Change Points in Time Series, Computational Statistics and Data Analysis, Impress.

Pelletier, B.R. and McMullen, R.M., 1972. Sedimentary patterns in the Bay of Fundy and Minas Basin, in Gray and Gashus (ed) Tidal Power. New York, Plenum Press. 153-187.

Qiu, H., Lam, N.S.N., Quatochi, D.A., Gamon, J.A., 1999, Fractal Characterization of Hyperspectral Imagery. Photogrammetric Engineering and Remote Sensing, 65, pp. 63–71.

Richardson, L.F., 1961. The Problem of Contiguity: An Appendix of Statistics of Deadly Quarrels: General Systems: Yearbook of the Society for General Systems Reserch 6, Ann Arbor, pp. 139–187.

Sharma, P., Byrne, S. 2010, Constraints on Titan's topography through fractal analysis of shorelines, Icarus, 209:723-737.

Schwimmer, A. R., 2008 A Temporal Geometric Analysis of Eroding Marsh Shorelines: Can Fractal Dimensions be Related to Process? Journal of Coastal Research, 24 (1), 152-158

Su, F., Gao, Y., Zhou, Ch., Yang, X., Fei, X. 2011, Scale effects of the continental coastline of China, Journal of Geographical Sciences, 21, 6:1101-111, DOI: 10.1007/s11442-011-0903-0.

Sun, W., XU, G.,Gong, P., and Liang,S., 2006, Fractal analysis of remotely sensed images:Areview of methods and applications, International Journal of Remote Sensing, 27 (22), 4963-4990.

Sung, Q.C, Chen, Y.C., 2004. Self-affinity Dimensions of Topography and Its Implications in Morphotectonics: An Example from Taiwan, Geomorphology, 62, 181–198.

Suteanu, C., 2000. Fractal-geometry-based analysis of microfabrics, in Kruhl J. (ed.), Proceedings of the Second European Workshop on the Analysis of Microfabrics in Geomaterials, Munich, 9-14 October 2000, Technical University of Munich, Tectonics and Material Fabrics Section, Vol. 2, 1.

Tate, N.J, 1998, Estimating the Fractal Dimension of Synthetic Topographic Surfaces. Computers and Geosciences, 24, pp. 325–334.

van Proosdij, D. 2005, Monitoring Seasonal Changes in Surface Elevation of Intertidal Environments near the Windsor Causeway. Final report prepared for the Nova Scotia Department of Transportation.

van Proosdij, D., Davidson-Arnott, R. G., & Ollerhead, J. 2006, Controls on spatial patterns of sediment deposition across a macro-tidal salt marsh surface over single tidal cycles. Estuarine, Coastal and Shelf Science, 69(1), 64-86.

van Proosdij, D., & Townsend, S. 2004, Spatial and temporal patterns of salt marsh colonization following causeway construction in the Bay of Fundy. Journal of Coastal Research, Special, (39).

van Proosdij, D. 2007. Intertidal Morphodynamics of the Avon River Estuary. Technical report for Nova Scotia Department of Transportation and Public Works, 120 p.

van Proosdij, D.; Milligan, T.; Bugden, G. and C. Butler. 2009. A Tale of Two Macro Tidal Estuaries: Differential Morphodynamic Response of the Intertidal Zone to

Causeway Construction. Journal of Coastal Research SI 56: 772-776. ISBN 0749-0258.

Wang, D., Wang, X., Wu, X., Gao, F. 2009, Method for fractal dimension calculation of the surface water in the Chaohu Lake Basin based on remote sensing images, Geospatial Information, 1, DOI: CNKI:SUN:DXKJ.0.2009-01-028.

Wang X., Zhong, X., Liu, S., Li, M., 2008, A non-linear technique based on fractal method for describing gully-head changes associated with land-use in an arid environment in China, Catena, Vol. 72, 1.

Walsh, J.S., Butler, R.D., Malanson, P.G., 1998. An Overview of Scale, Pattern, Process Relationships in Geomorphology: A Remote Sensing and GIS Perspective, Geomorphology 21, 183-205.

Watson D.F., 1992, Contouring: a guide to the analysis and display of spatial data. Oxford, Pergamon.

Wechsler, S. P. (2007). Uncertainties associated with digital elevation models for hydrologic applications: a review. Hydrology and Earth System Sciences Discussions, 11(4), 1481-1500.

Yan, C., Chao, W., Fuqiang, Y., Hui, L., Ming, Li 2011, Shape analysis of indoor free settling particulate matters, Bioinformatics and Biomedical Engineering, 5th Conference, 1-4, doi: 10.1109/icbbe.2011.5781256.

Zaady, E., Dody, A., Weuner, D., Barkai, D., Offer, Z.Y. 2009, A comprehensive method for aeolian particle granulometry and micromorphology analyses, Environmental Monitoring and Assessment, 155, 1:169-175.